Electronic Supplementary Information (ESI)

An N-heterocyclic carbene functional covalent organic framework for Knoevenagel condensation reaction and γ-Butyrolactone synthesis under room temperature

Wenyao Zhang, † Biying Wang, † Shulei Feng, Huijun Feng, Junhua Bai, Junwen Wang*

Key Laboratory of Magnetic Molecules and Magnetic Information Materials of Ministry of Education, School of Chemistry and Materials Science, Shanxi Normal University, TaiYuan 030031, China.

E-mail: wangjunwen2013@126.com

Table of Contents

S1. General considerations

All solvents meso-tetra(p-formylphenyl)porphyrin (*p*-Por-CHO) and other reagents were of reagent grade quality. ^{1}H NMR and ^{13}C NMR spectra were obtained by using Bruker Avance III HD (600 MHz) spectrometers unless noted otherwise. ^{1}H NMR and ^{13}C NMR chemical shifts were based on the residual solvent peaks as the internal standard (2.50 ppm for DMSO-d_6, 7.26 ppm for $CDCl_3$ for ^{1}H NMR; (39.52 ppm for DMSO-d_6, 77.16 ppm for $CDCl_3$ for ^{13}C NMR). Solid-state cross-polarisation magicangle spinning (CP/MAS) ^{13}C NMR spectrum was measured on an Agilent DD2 600 Solid NMR 3 System with 3.2mm zirconia rotors. The fourier transform infrared (FT-IR) spectra were measured by the using of KBr pellets in the range of 4000-400 cm^{-1} on a Varian 660-IR spectrometer. Powder X-ray diffraction (PXRD) measurements were taken on a Rigaku Ultima IV-185 diffractometer with Cu-filtered Kα radiation (λ = 1.5404 Å). Thermogravimetric analysis (TGA) measurement was measured at a NETZSCH DSC 200F3 instrument. N_2 sorption isotherm was carried out on a liquid nitrogen bath at 77 K. Transmission electron microscopy (TEM) graphs were obtained on a JEOL JEM-2100 instrument. X-ray photoelectron spectroscopy (XPS) spectrum was taken on a Thermo K-Alpha^{+}scientific electron spectrometer using Al Kα radiation.

S2. Syntheses

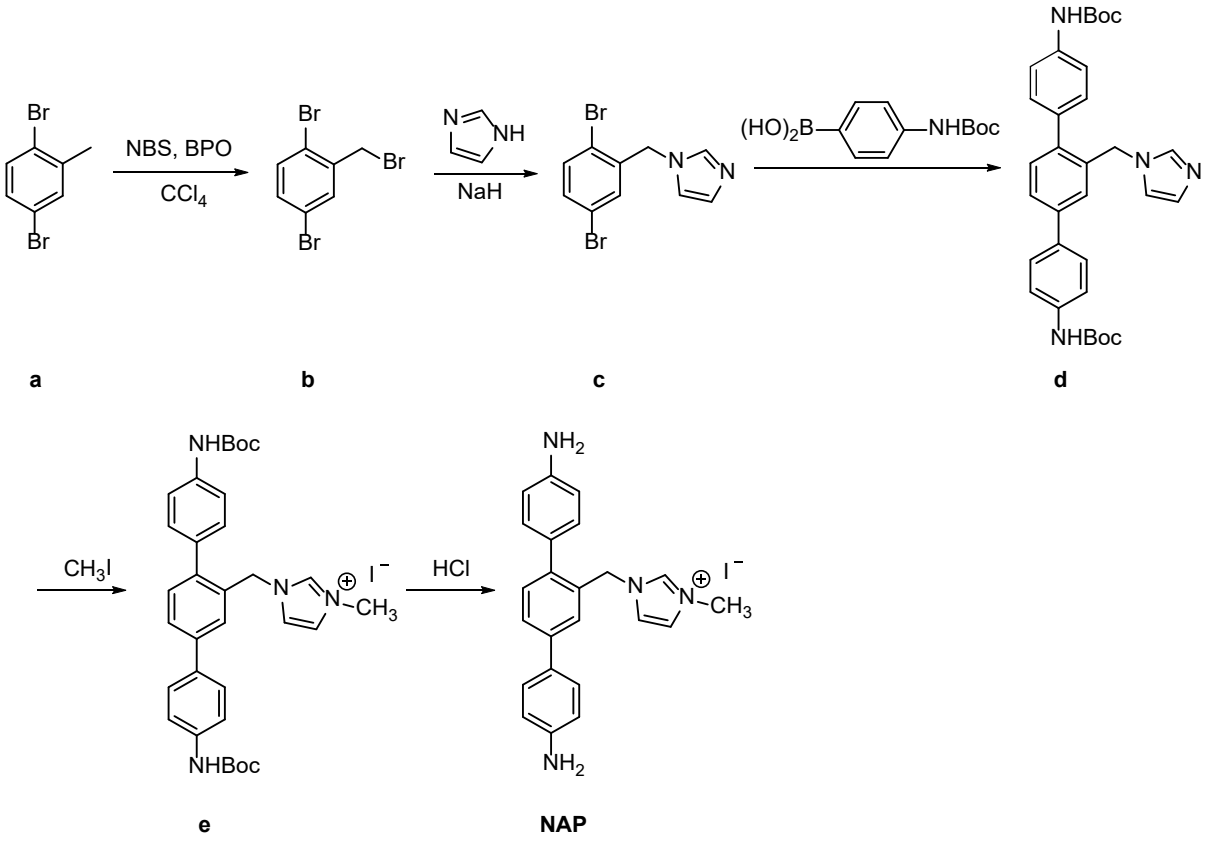

Scheme S1. Synthesis of monomer **NAP**.

Synthesis of α,2,5-Tribromotoluene (b)

Compound **b** was prepared according to reported literature procedures.[1]

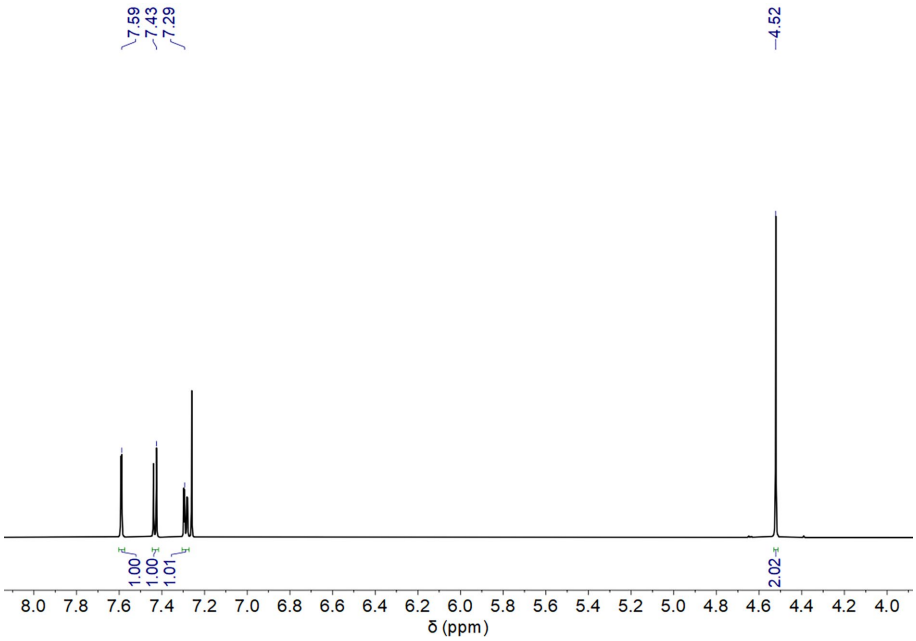

Fig. S1 ^{1}H NMR spectrum (600 MHz, $CDCl_3$, 298 K) of **b**.

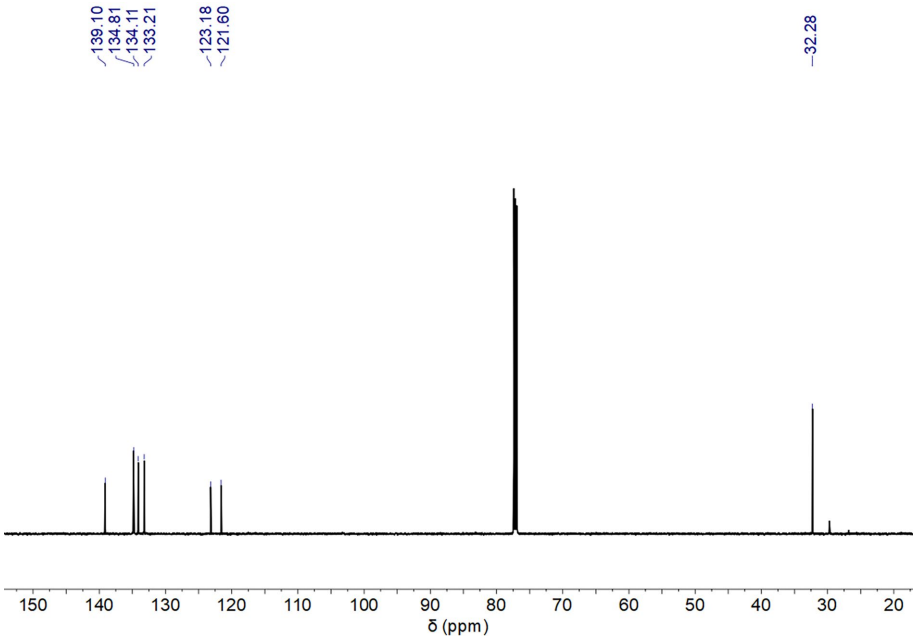

Fig. S2 ^{13}C NMR spectrum (150 MHz, $CDCl_3$, 298 K) of **b**.

Synthesis of 1,4-Dibromo-2-imidazolemaethyl Benzene (c)

Imidazole (0.14 g, 2 mmol) dissolved in 10 ml anhydrous THF in a 3-neck round-bottom flask then NaH (0.2 g, 4 mmol) was added and stirred heated at 60℃ for 30 minutes in a nitrogen atmosphere and. Then compound **b** (0.4 g, 1.2 mmol) was added and the mixture was stirred heated for 6 hours. When the

mixture cooled to room temperature 10 ml H_2O was added slowly to quench reaction. Vacuum distillation of the liquid and compound **c** (342 mg, 89%) was obtained. ^{1}H NMR ($CDCl_3$): δ 7.55 (s, 4H), 7.42 (d, 1H), 7.30 (dd, 1H), 7.11 (s, 1H), 6.96 (d, 1H), 6.92 (d, 1H), 5.15 (s, 1H) ppm; ^{13}C NMR: δ 137.74, 137.70, 134.46, 132.95, 131.69, 130.25, 122.09, 121.41, 119.31, 50.35 ppm.

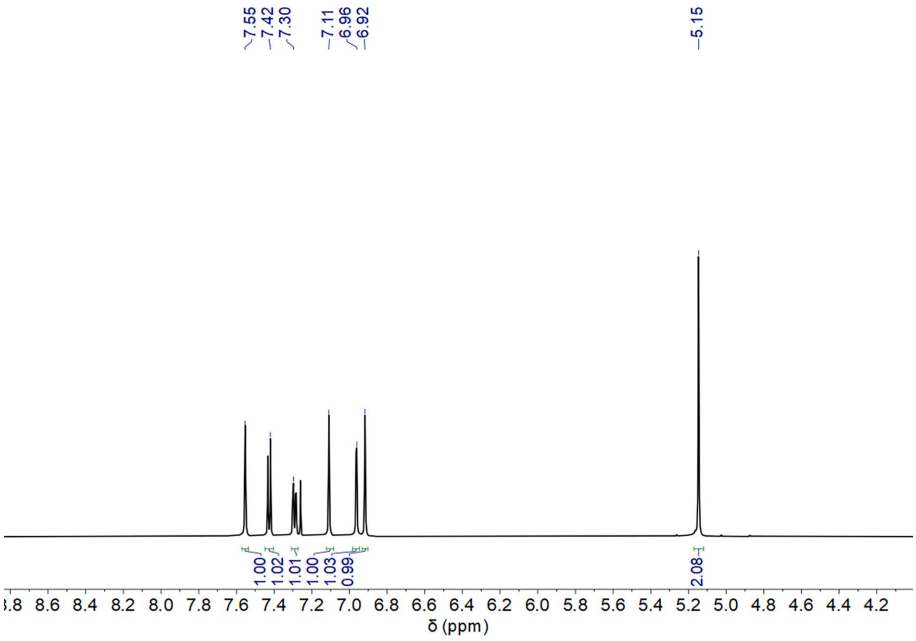

Fig. S3 ^{1}H NMR spectrum (600 MHz, $CDCl_3$, 298 K) of **c**.

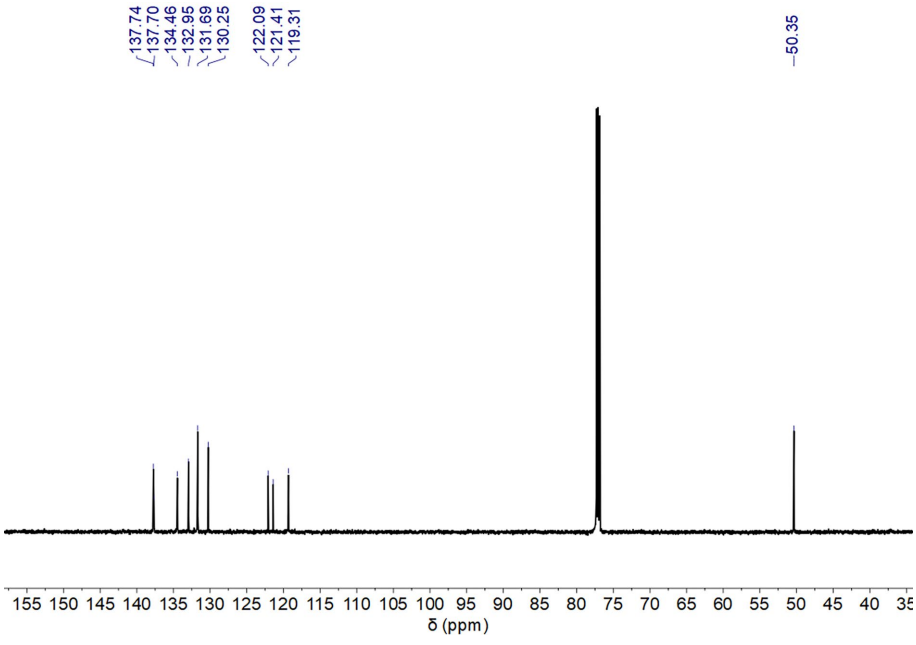

Fig. S4 ^{13}C NMR spectrum (150 MHz, $CDCl_3$, 298 K) of **c**.

Synthesis of (2,5-Dibromophenyl)methyl-1*H*-imidazolium (d)

Compound **c** (300 mg, 0.95 mmol), 4-Boc-Aminophenyl)Boronic Acid (660 mg, 2.78 mmol), $NaCO_3$ (800 mg) and $Pd(PPh_3)_4$ (80 mg, 0.07mmol) were mixed in 35 ml toluene and heated at 95℃ for 3 days under nitrogen atmosphere. Vacuum distillation of toluene, the solid was dissolved in ethyl acetate and washed with H_2O. Then vacuum distillation of ethyl acetate and the crude product was recrystallization with ethyl acetate (5 ml) and petroleum ether (5 ml) to obtained compound **d** (400 mg, 80%). ^{1}H NMR (DMSO-d_6): δ 9.53 (s, 1H), 9.48 (s, 1H), 7.57 (m, 5H), 7.41 (s, 1H), 7.35 (s, 1H), 7.27 (d, 1H), 7.26 (d, 2H), 7.93 (s, 1H), 6.85 (s, 1H), 5.22 (s, 2H), 1.50 (s, 9H), 1.49 (s, 9H) ppm; ^{13}C NMR: δ 152.83, 152.76, 139.32, 139.30, 139.07, 139, 137.4, 135.20, 133.13, 133.01, 130.81, 129.33, 128.57, 126.76, 126.10, 125.62, 119.44, 118.49, 117.97, 79.17, 47.73, 28.13 ppm.

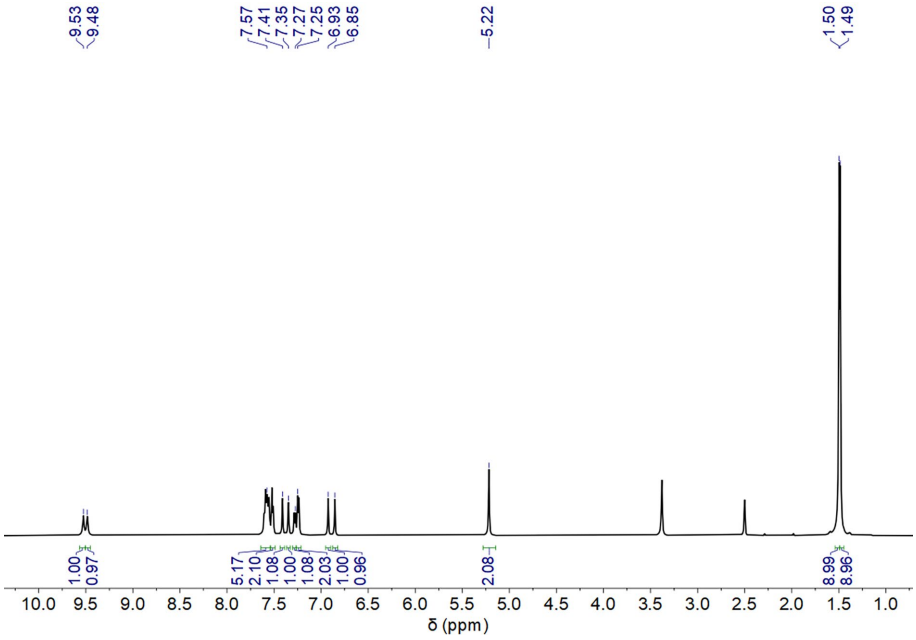

Fig. S5 ^{1}H NMR spectrum (600 MHz, DMSO-d_6, 298 K) of **d**.

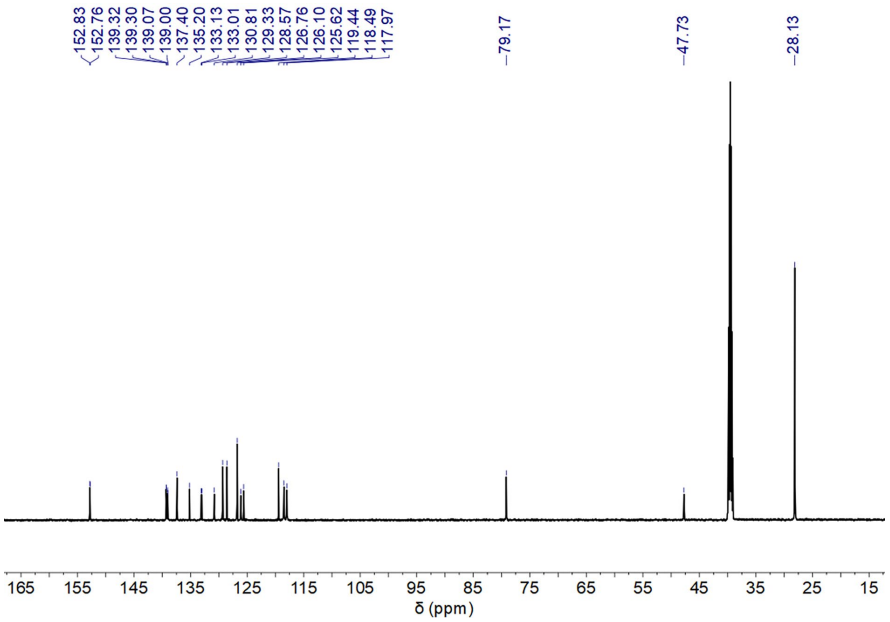

Fig. S6 ^{13}C NMR spectrum (150 MHz, DMSO-d_6, 298 K) of **d**.

Synthesis of (2,5-Dibromophenyl)methyl-1*H*-imidazolium (e)

Compound 4 (400 mg, 0.74 mmol) and iodomethane (1.2 ml) were dissolved in 10ml THF and stirred for 1 hour at room temperature. Compound **e** (500 mg) was filtered and collected in 99% yield. ^{1}H NMR (DMSO-d_6): δ 9.58 (s, 1H), 9.56 (s, 1H), 8.78 (s, 1H), 7.77 (d-d, 1H), 7.73 (s, 1H), 7.69 (s, 1H), 7.68 (m, 2H), 7.64 (d, 2H), 7.61 (d, 2H), 7.45 (t, 1H), 7.40 (d, 1H), 7.24 (d, 2H), 5.48 (s, 2H), 3.81 (s, 3H), 1.56 (s, 9H), 1.55 (s, 9H) ppm; ^{13}C NMR: δ 152.85, 152.78, 139.99, 139.46, 139.35, 139.15, 136.76, 132. 67, 132.62, 132.14, 131.17, 129.01, 127.46, 126.99, 126.67, 123.71, 122.30, 118.46, 118.11, 79.28, 52.84, 35.71, 28.15 ppm.

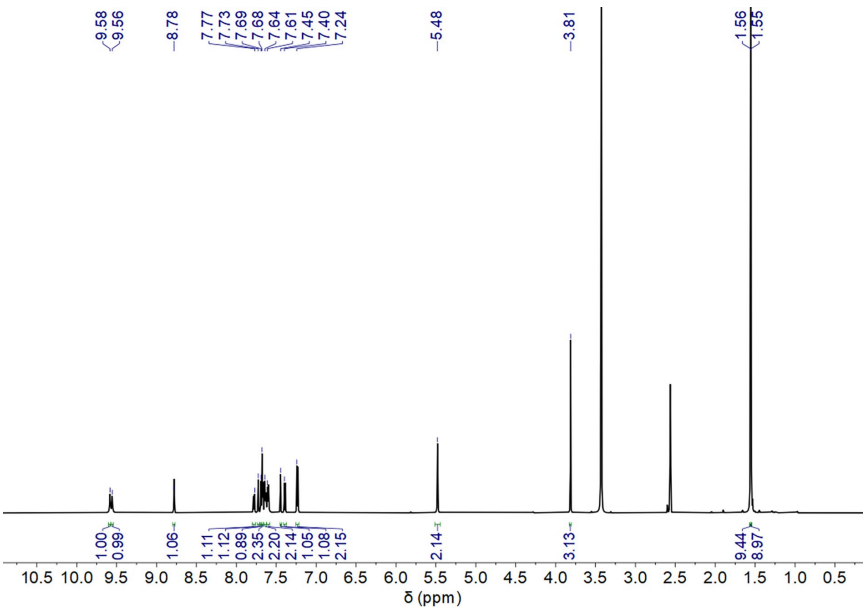

Fig. S7 ^{1}H NMR spectrum (600 MHz, DMSO-d_6, 298 K) of **d**.

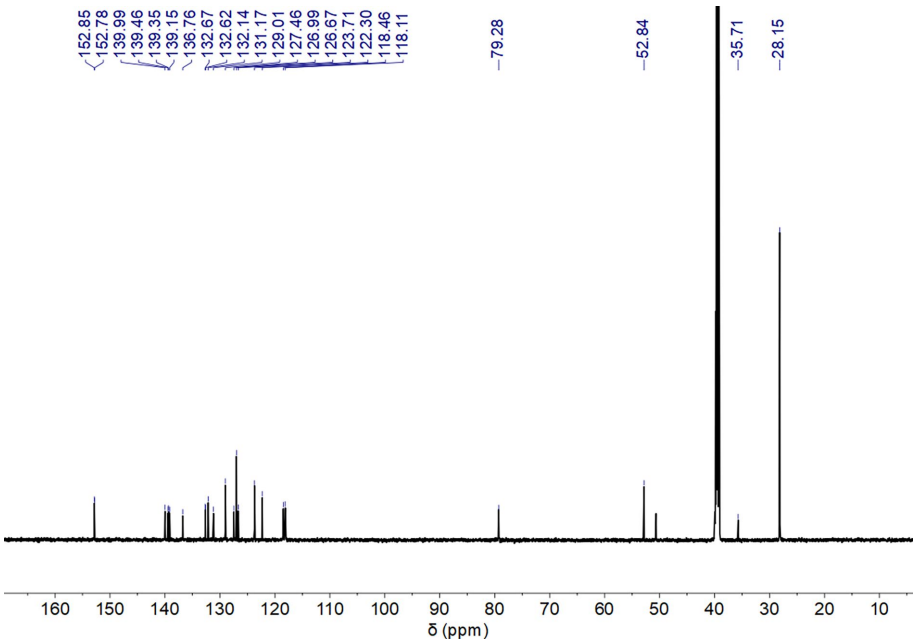

Fig. S8 ^{13}C NMR spectrum (150 MHz, DMSO-d_6, 298 K) of **d**.

Synthesis of monomer NAP

Compound **e** (400 mg, 0.83 mmol) was dissolved in 10 ml hydrogen chloride-ethanol solution and stirred overnight, the mixture were evaporator and collected the precipitate to obtained compound **NAP** (270 mg, 94.5%). ^{1}H NMR (DMSO-d_6): δ 8.76 (s, 1H), 7.81 (m, 3H), 7.74 (s, 1H), 7.62 (s, 1H), 7.43 (m, 8H), 5.47 (s, 2H), 3.78 (m, 7H) ppm; ^{13}C NMR: δ 139.88, 139.11, 136.82, 132.43, 131.20, 129.90, 128.06, 128.03, 127.23, 123.77, 123.24, 122.94, 122.31, 50.48, 35.87 ppm.

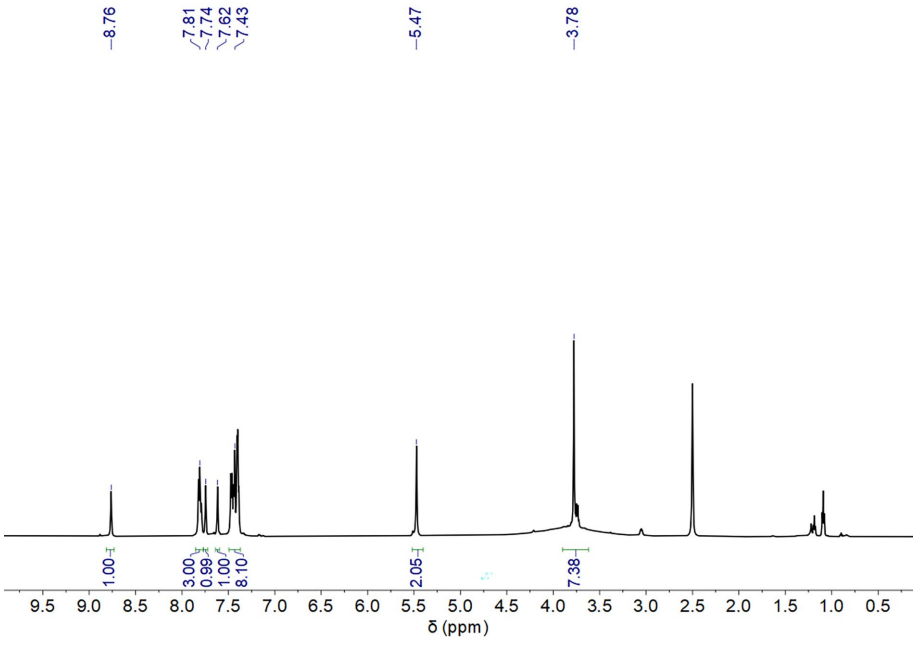

Fig. S9 ^{1}H NMR spectrum (600 MHz, DMSO-d_6, 298 K) of monomer **NAP**.

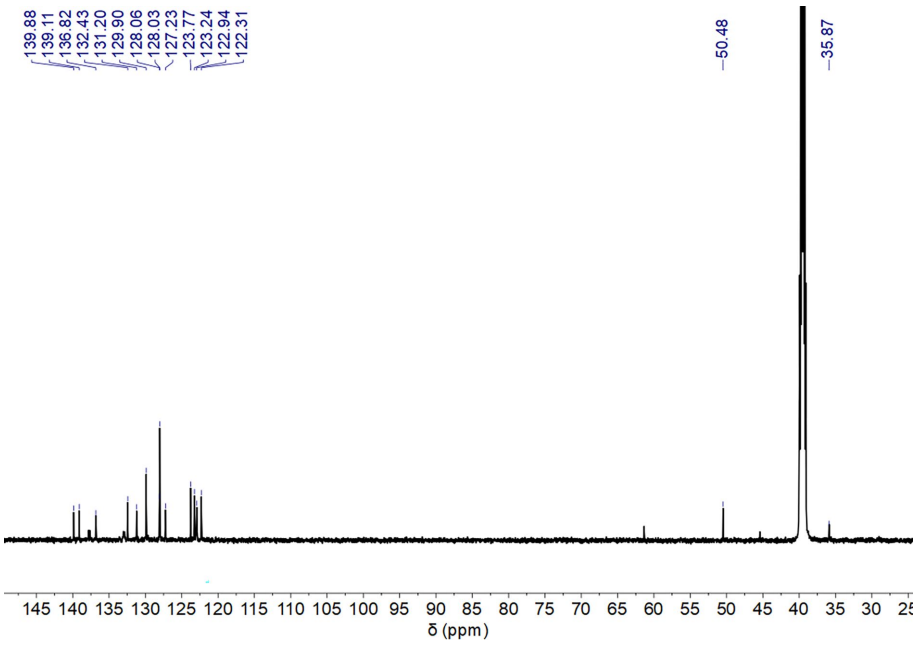

Fig. S10 ^{13}C NMR spectrum (150 MHz, DMSO-d_6, 298 K) of monomer **NAP**.

Synthesis of Por-NHC-COF:

To prepare **Por-NHC-COF**, monomer **NAP** (16 mg, 0.034 mmol) and monomer ***p*-Por-CHO** (12 mg, 0.017 mmol, 0.5 equiv) were mixed in a pyrex tube. Then two solvents, 2 ml of DMSO and 0.25 mL of H_2O, and 0.25 ml of aqueous acetic acid (6 M) were added to the mixture, the mixture was sonicated for 30 minutes until the precipitation was dissolved completely. The tube was subjected to freeze-pump-thaw cycles and flame-sealed under nitrogen atmosphere and then heated at 120℃ for 3 days. After cooling, the power was collected and washed dichloromethane, methanol, ethanol and DMF and then vacuum dried at 80℃ for 12 hours, yielding a dark purple powder (16.8 mg, 61%).

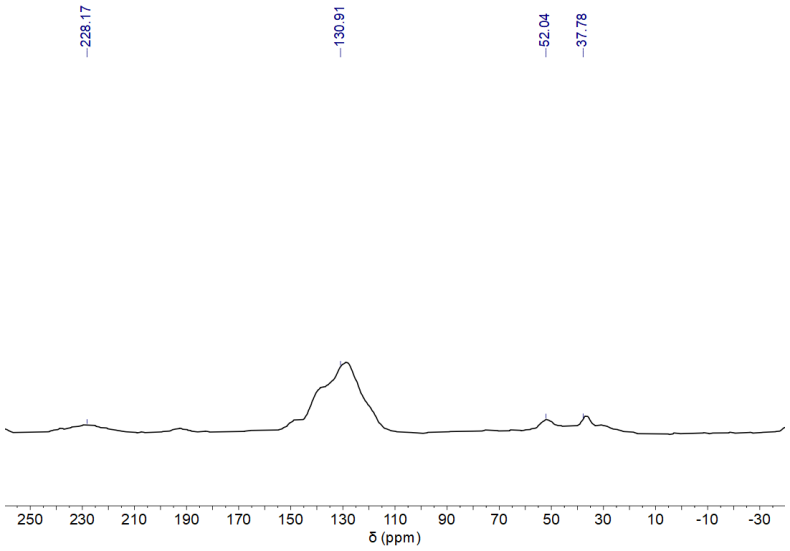

Fig. S11 ^{13C} CP/MAS NMR spectrum of monomer **Por-NHC-COF**.

S3. Characterizations of Por-NHC-COF

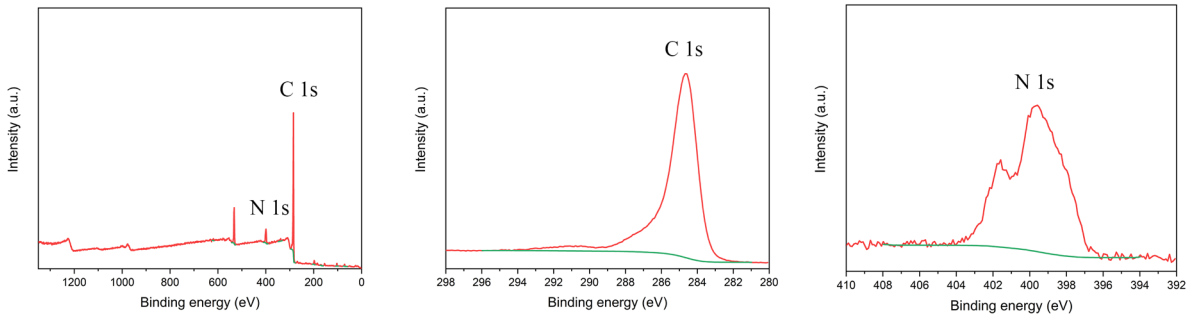

Fig. S12 XPS profiles of **Por-NHC-COF**.

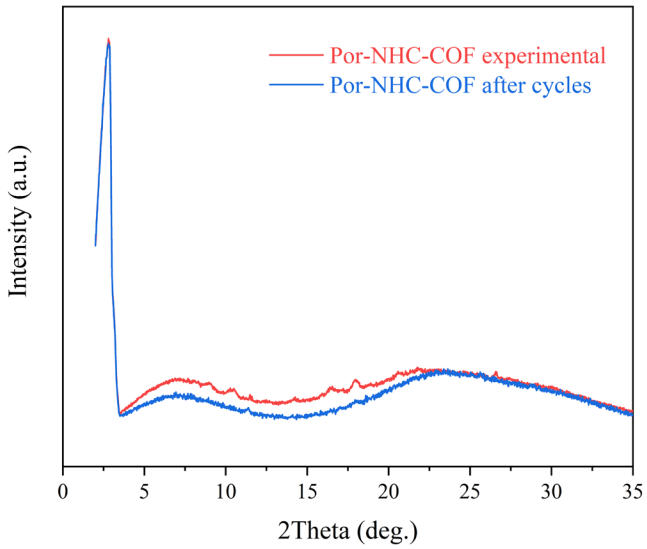

Fig. S13 PXRD spectra of **Por-NHC-COF** (red) before and after six catalytic cycles (blue).

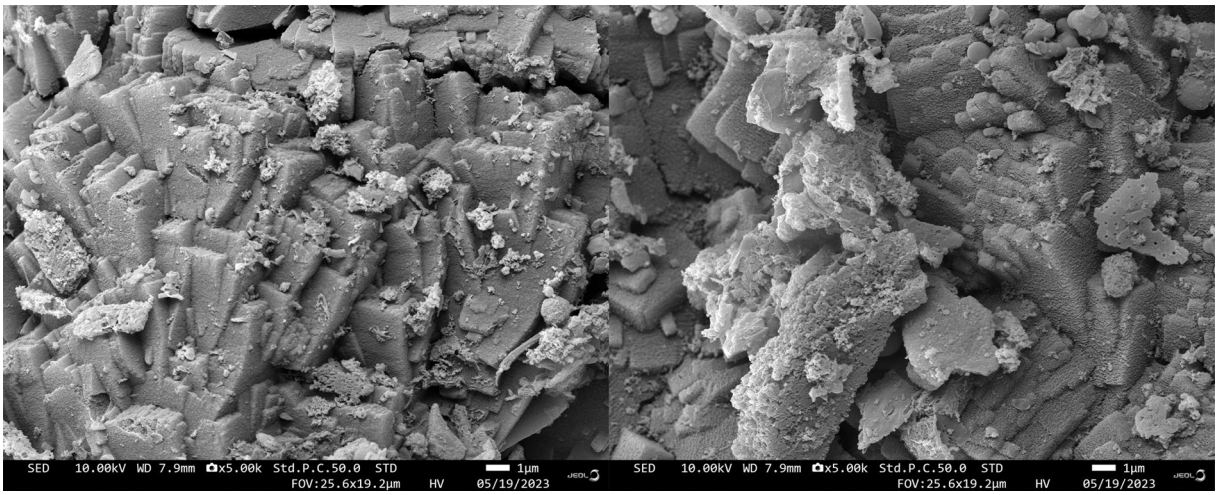

Fig. S14 SEM images of **Por-NHC-COF**.

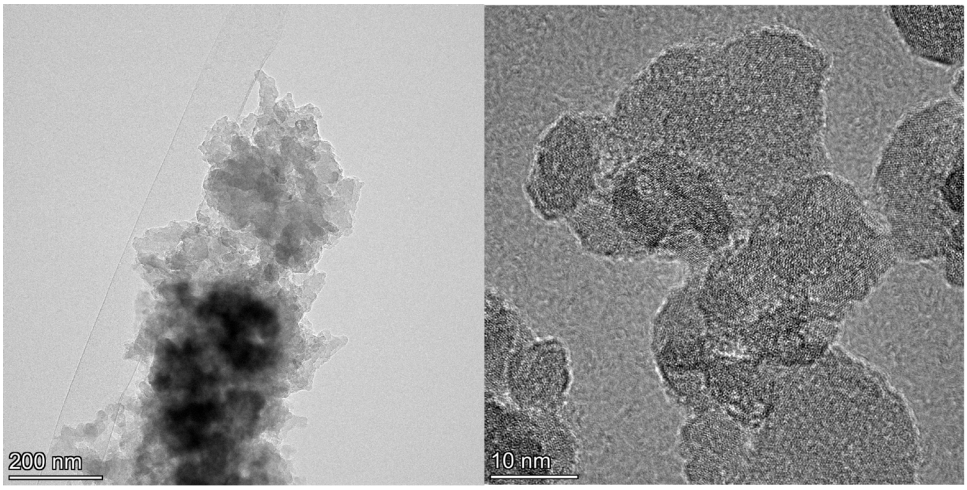

Fig. S15 TEM images of **Por-NHC-COF**.

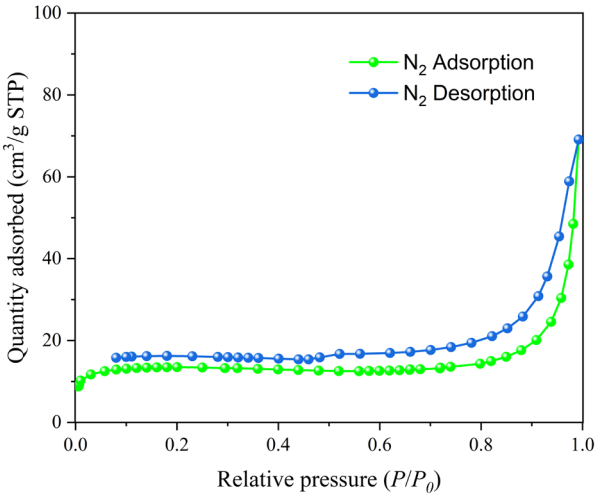

Fig. S16 Nitrogen adsorption-desorption isotherm profiles of **Por-NHC-COF**.

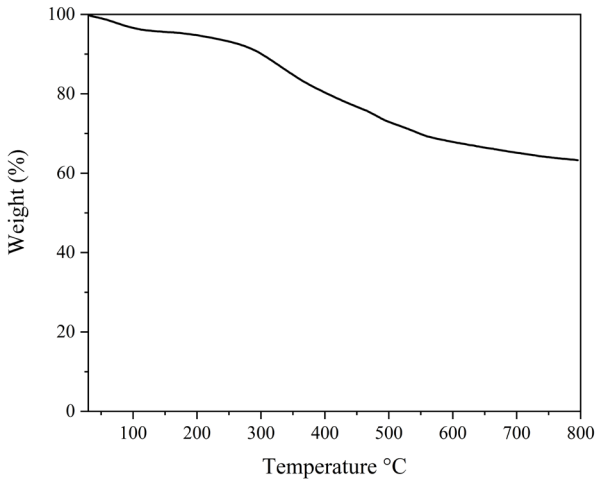

Fig. S17 TGA curve of **Por-NHC-COF**.

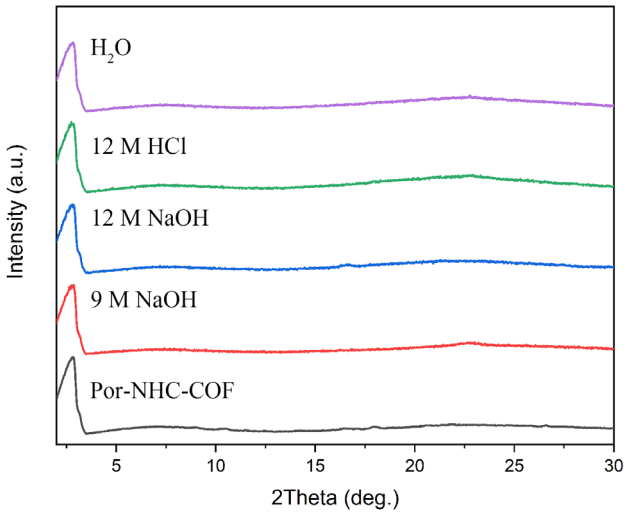

Fig. S18 PXRD patterns of **Por-NHC-COF** after treatment under different conditions.

S4. Molecular dynamic (MD) simulations

Molecular dynamic (MD) simulations were respectively applied to investigate the interaction energy and XRD of AA and AB bilayer stacking **Por-NHC-COF**. All structure optimization and energy calculation were carried out by Forcite module with COMPASS III force field[2, 3] in MS 2020[4]. Van der Waals and Coulomb interactions were respectively considered by atom based and Ewald methods with a cut-off value of 15.5 Å. Furthermore, the simulated XRD was obtained by Reflex Power Diffraction tool in Reflex module of MS.

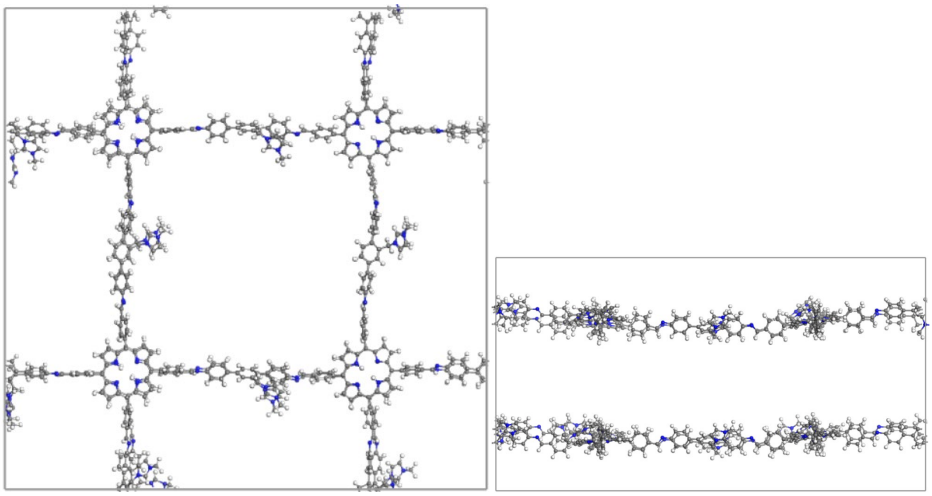

Fig. S19 AA stacking structure and side view of ideal AA stacking structure, the total energy is 943.076 kcal/mol.

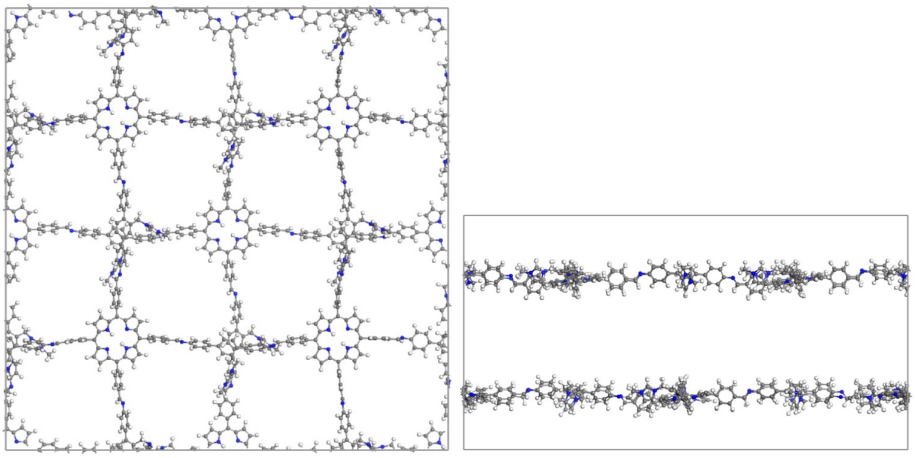

Fig. S20 AB stacking structure and side view of ideal AB stacking structure, the total energy is 989.409 kcal/mol.

S5. NMR spectra of products

Table S1. Substrate Scope of Knoevenagel condensation reaction catalyzed by **Por-NHC-COF**.

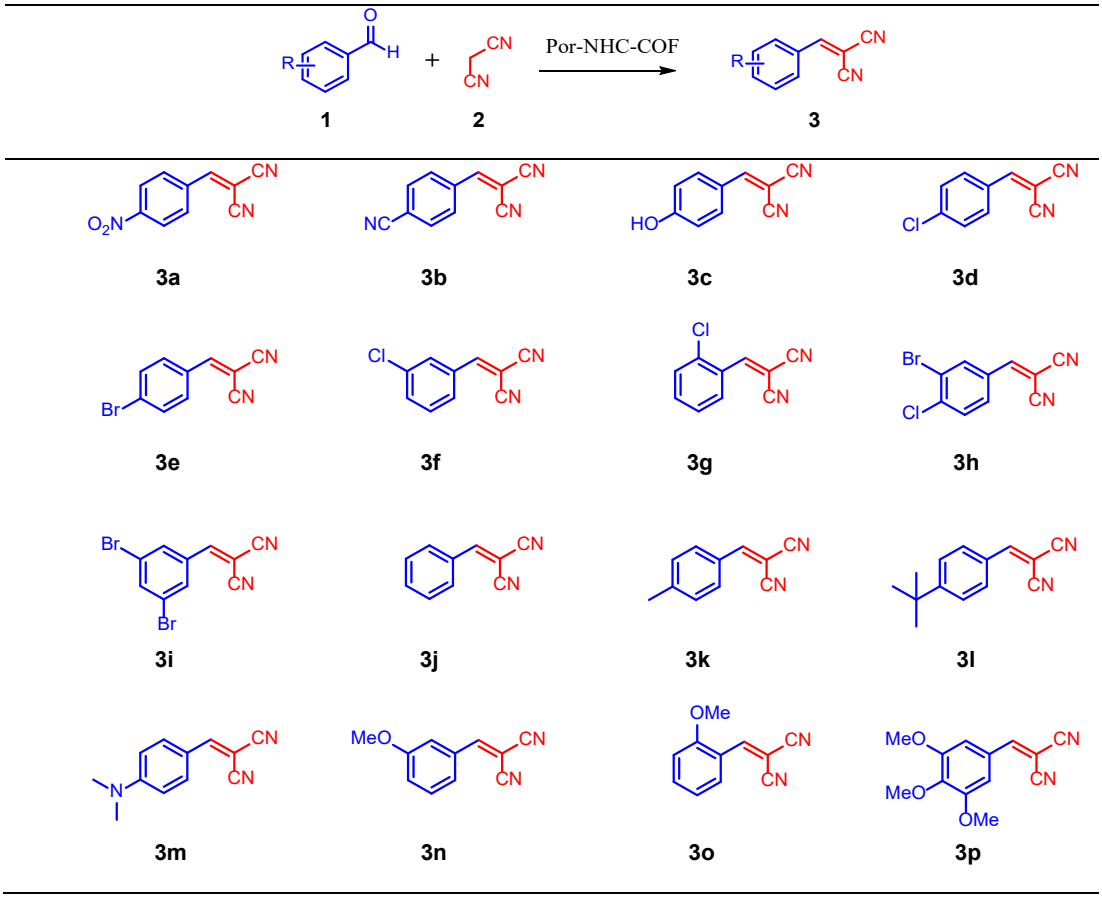

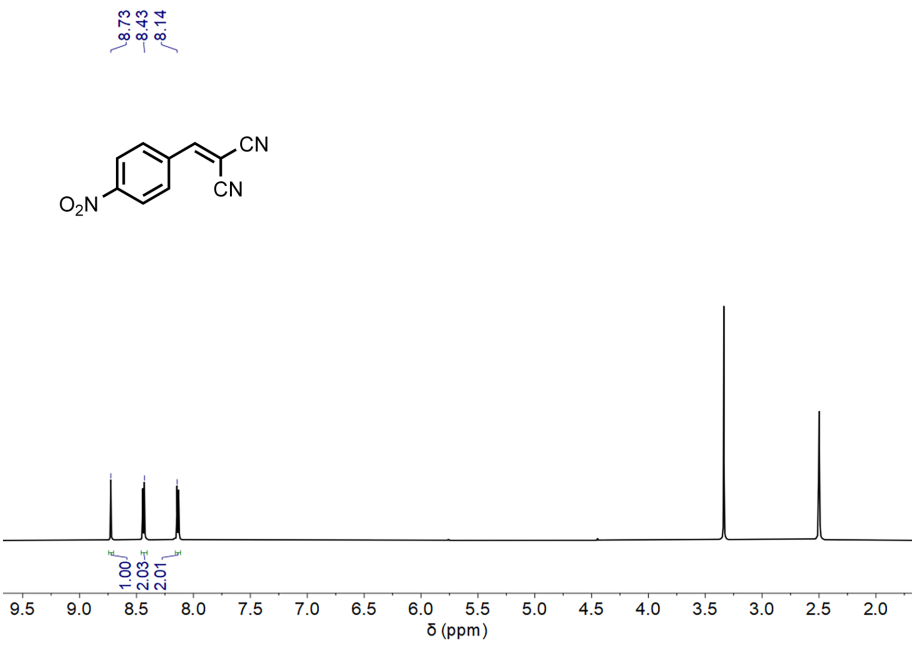

Fig. S21 ^{1}H NMR spectrum (600 MHz, DMSO-d_6, 298 K) of **3a**.

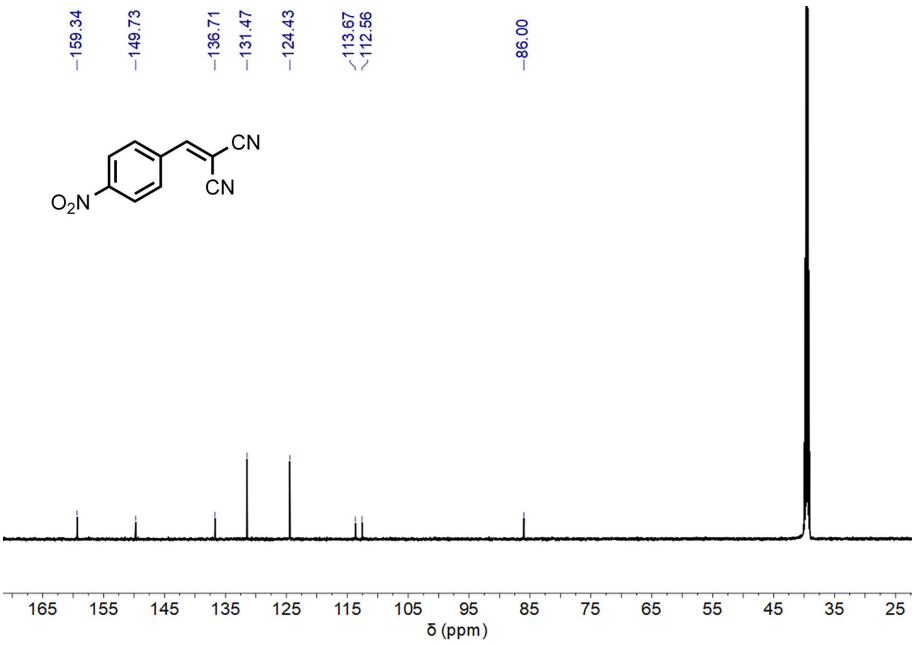

Fig. S22 ^{13}C NMR spectrum (150 MHz, DMSO-d_6, 298 K) of **3a**.

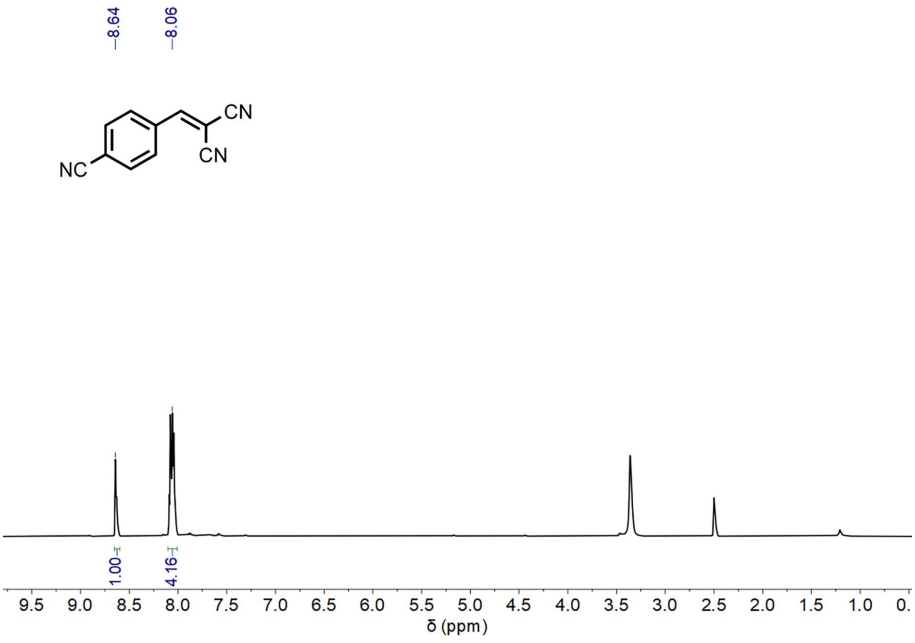

Fig. S23 ^{1}H NMR spectrum (600 MHz, DMSO-d_6, 298 K) of **3b**.

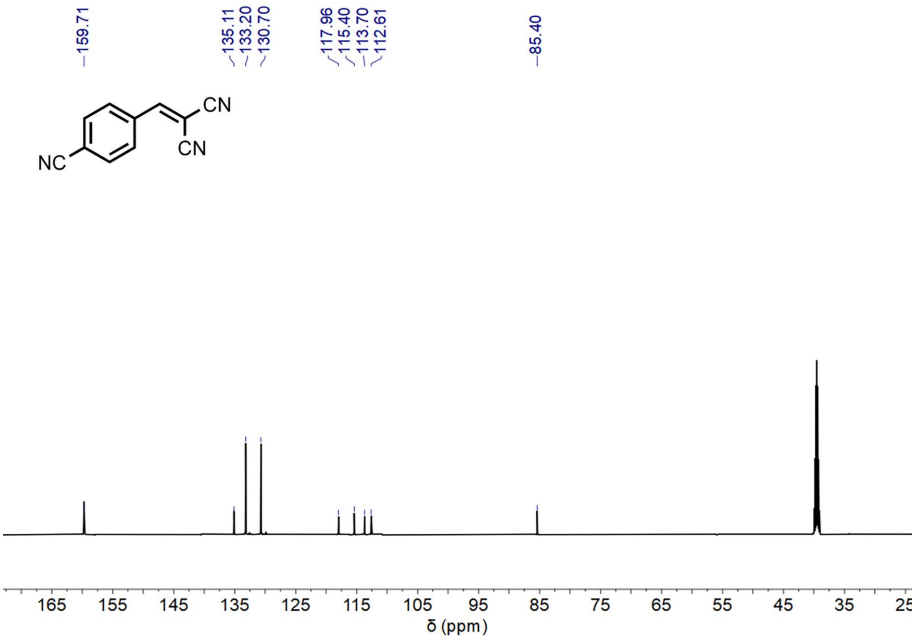

Fig. S24 ^{13}C NMR spectrum (150 MHz, DMSO-d_6, 298 K) of **3b**.

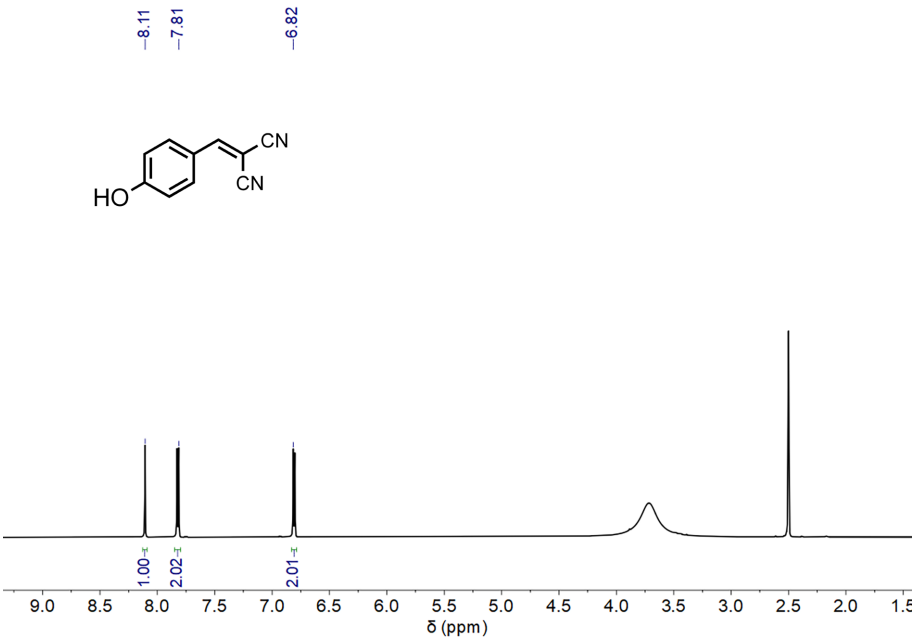

Fig. S25 ^{1}H NMR spectrum (600 MHz, DMSO-d_6, 298 K) of **3c**.

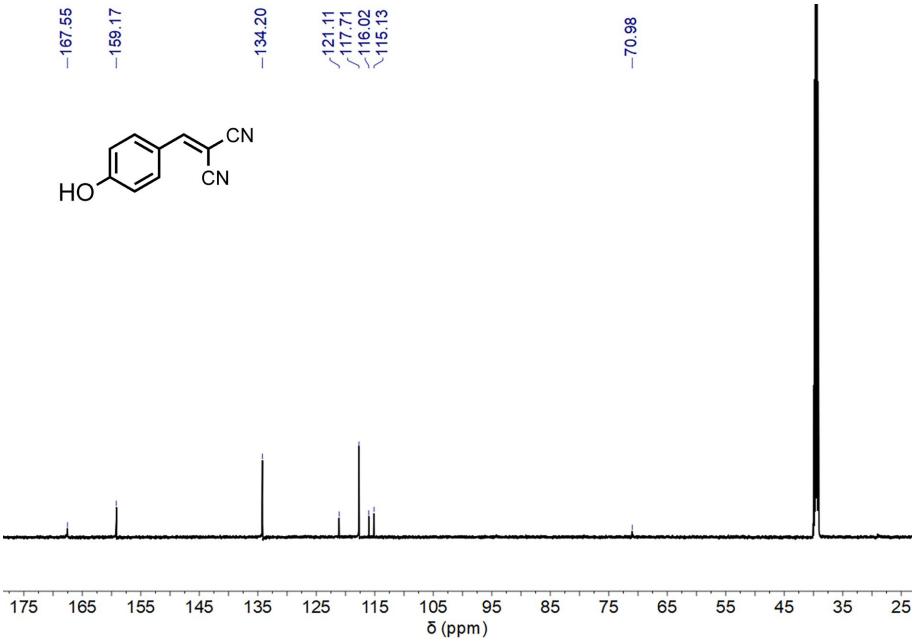

Fig. S26 ^{13}C NMR spectrum (150 MHz, DMSO-d_6, 298 K) of **3c**.

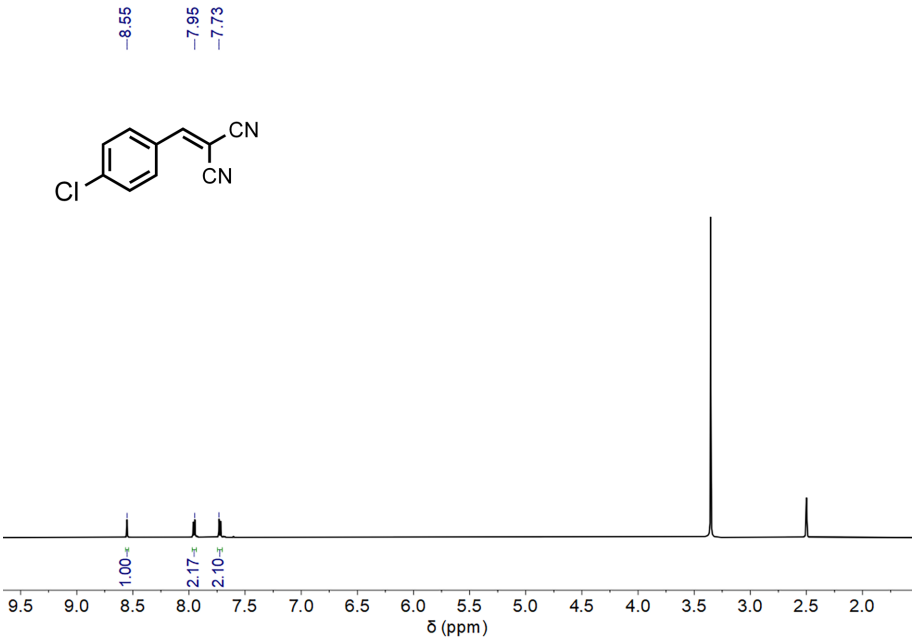

Fig. S27 ^{1}H NMR spectrum (600 MHz, DMSO-d_6, 298 K) of **3d**.

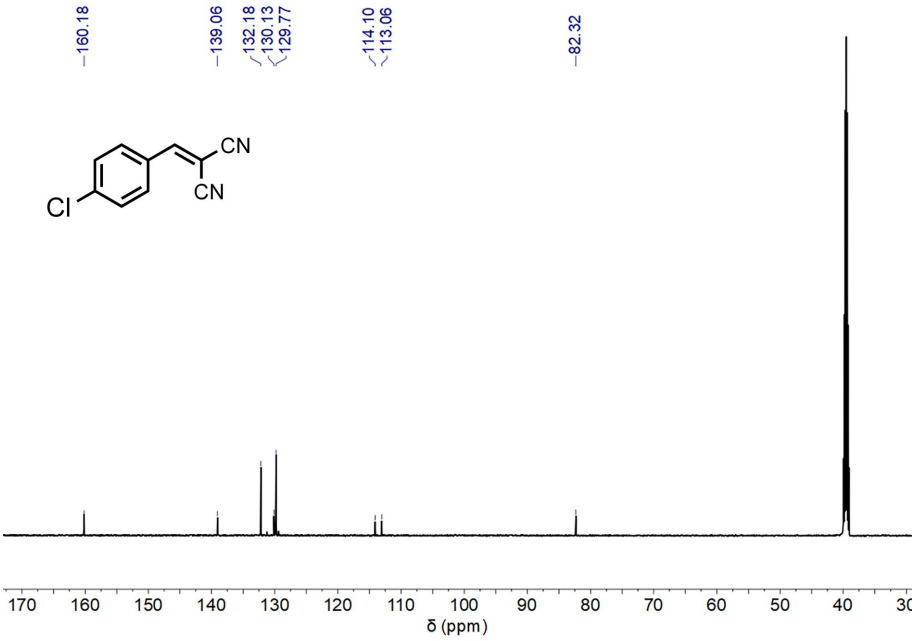

Fig. S28 ^{13}C NMR spectrum (150 MHz, DMSO-d_6, 298 K) of **3d**.

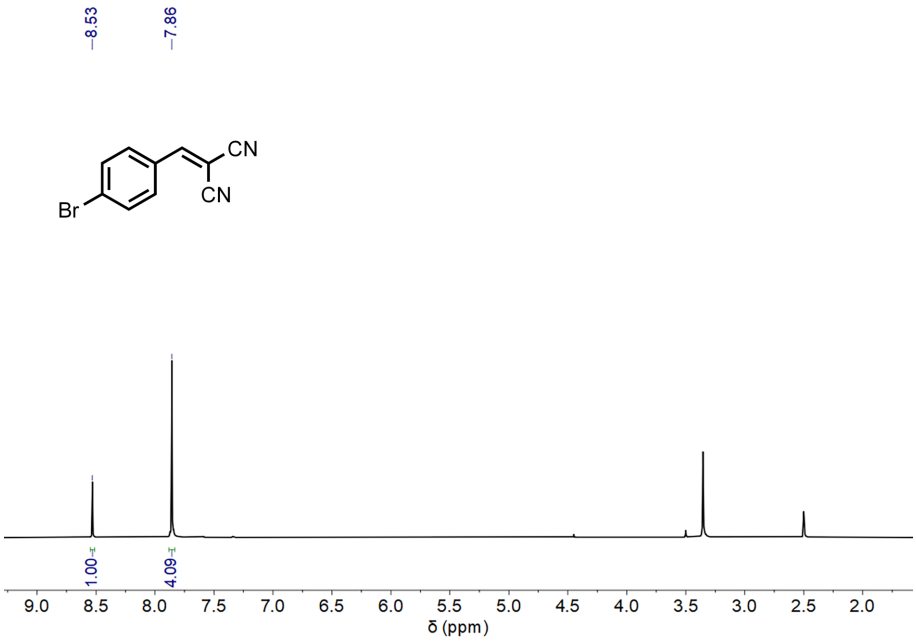

Fig. S29 ^{1}H NMR spectrum (600 MHz, DMSO-d_6, 298 K) of **3e**.

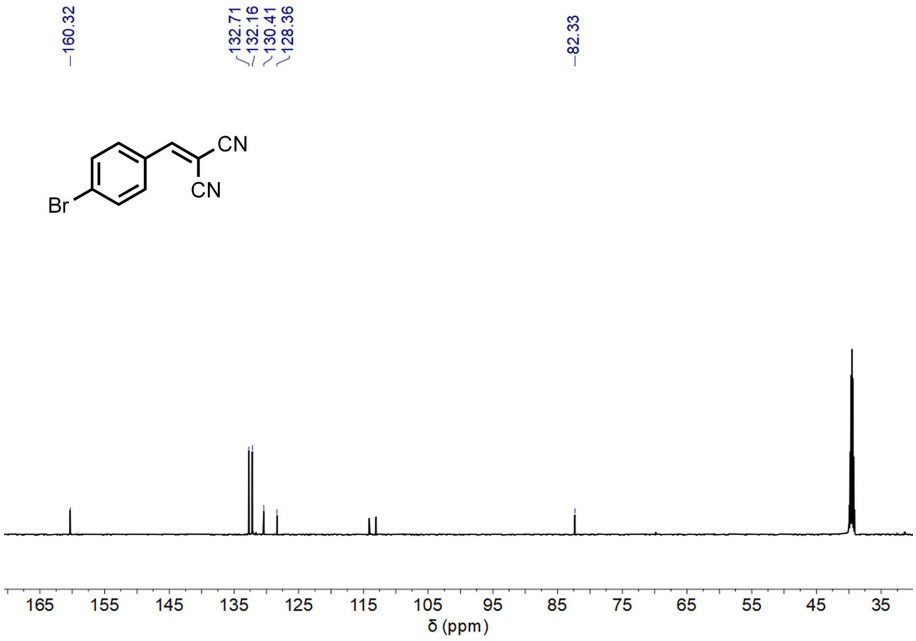

Fig. S30 ^{13}C NMR spectrum (150 MHz, DMSO-d_6, 298 K) of **3e**.

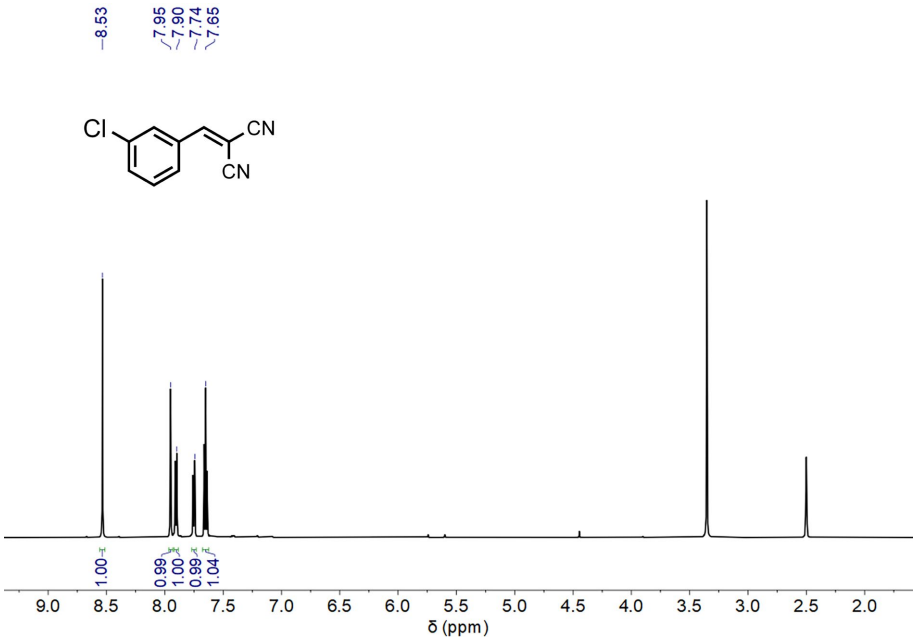

Fig. S31 ^{1}H NMR spectrum (600 MHz, DMSO-d_6, 298 K) of **3f**.

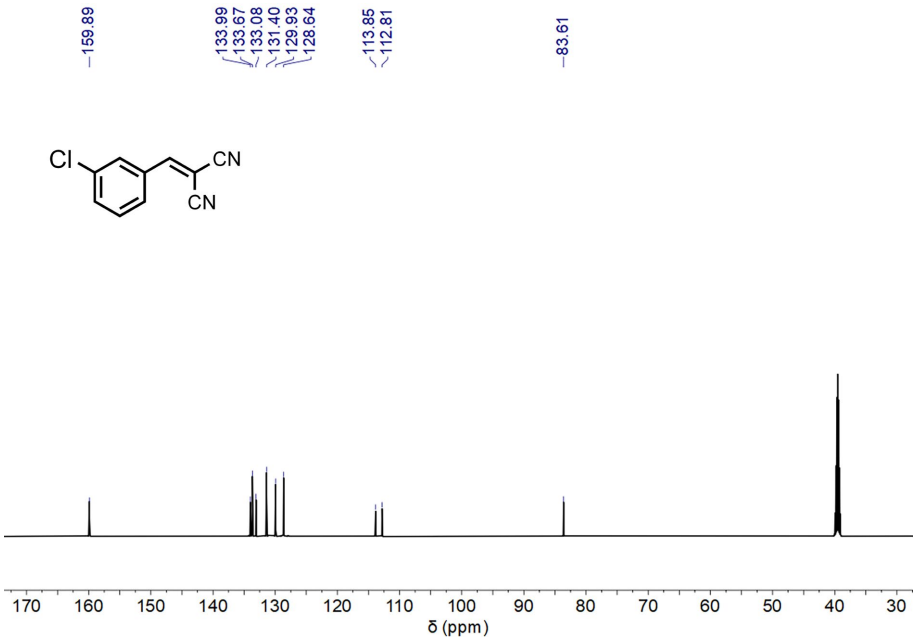

Fig. S32 ^{13}C NMR spectrum (150 MHz, DMSO-d_6, 298 K) of **3f**.

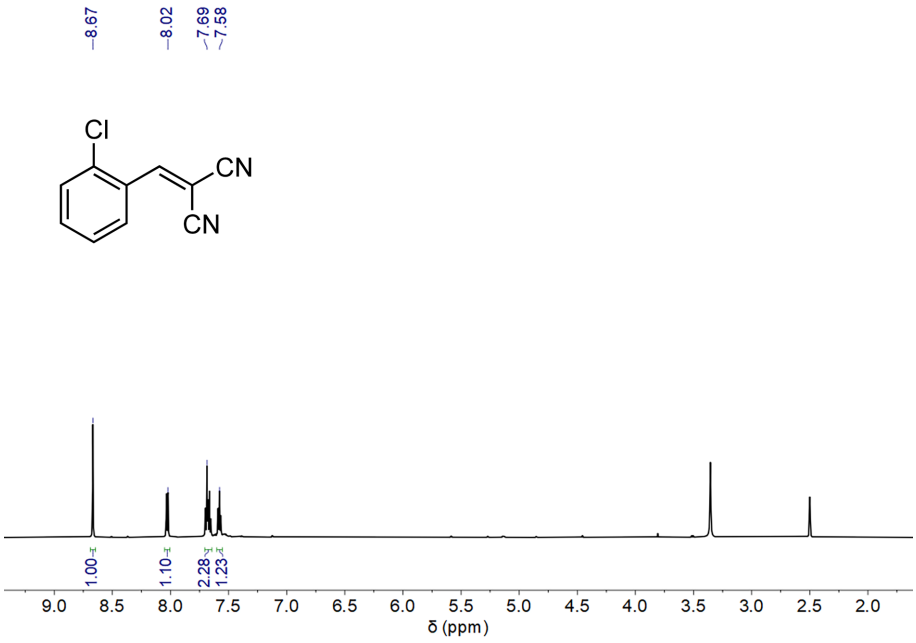

Fig. S33 ^{1}H NMR spectrum (600 MHz, DMSO-d_6, 298 K) of **3g**.

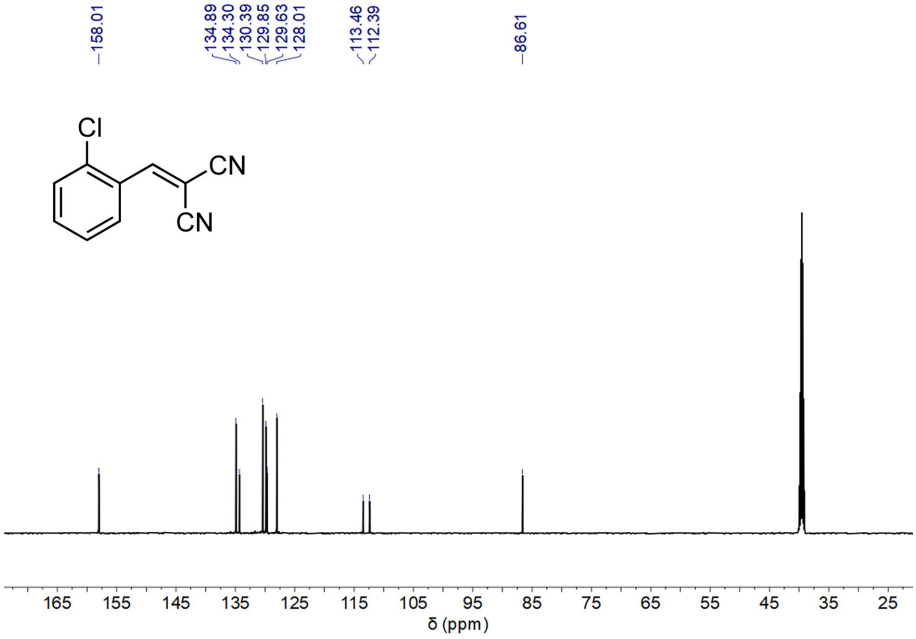

Fig. S34 ^{13}C NMR spectrum (150 MHz, DMSO-d_6, 298 K) of **3g**.

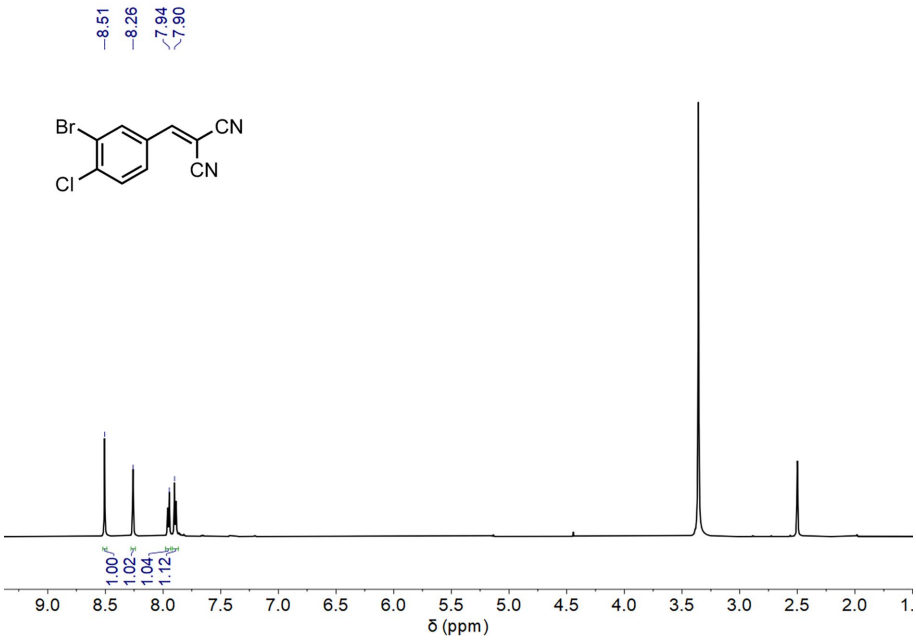

Fig. S35 ^{1}H NMR spectrum (600 MHz, DMSO-d_6, 298 K) of **3h**.

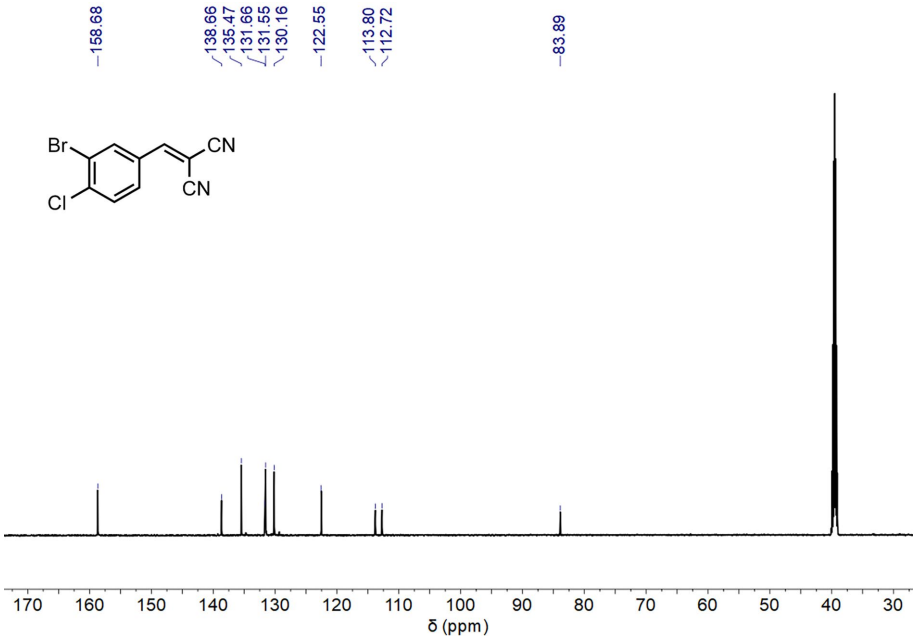

Fig. S36 ^{13}C NMR spectrum (150 MHz, DMSO-d_6, 298 K) of **3h**.

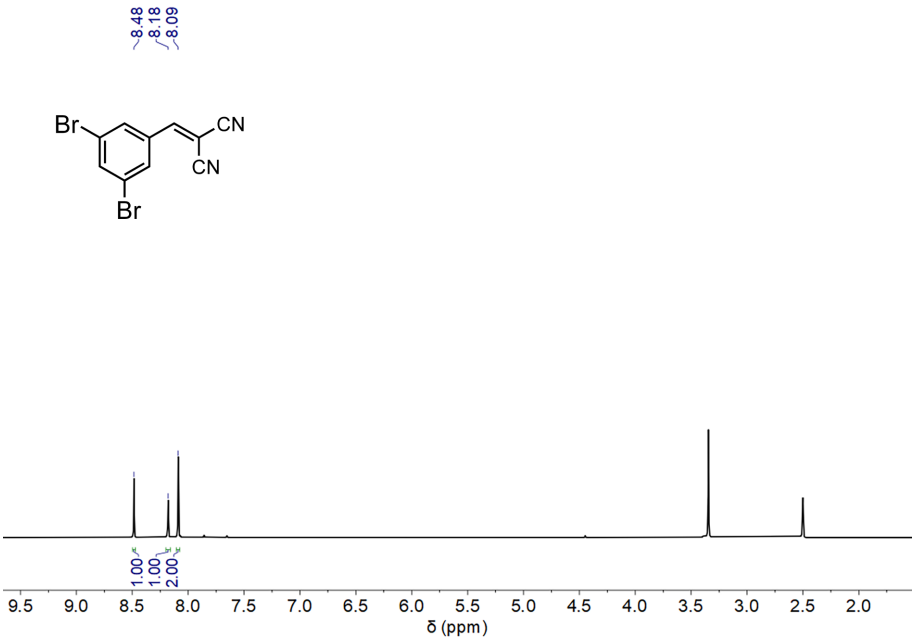

Fig. S37 ^{1}H NMR spectrum (600 MHz, DMSO-d_6, 298 K) of **3i**.

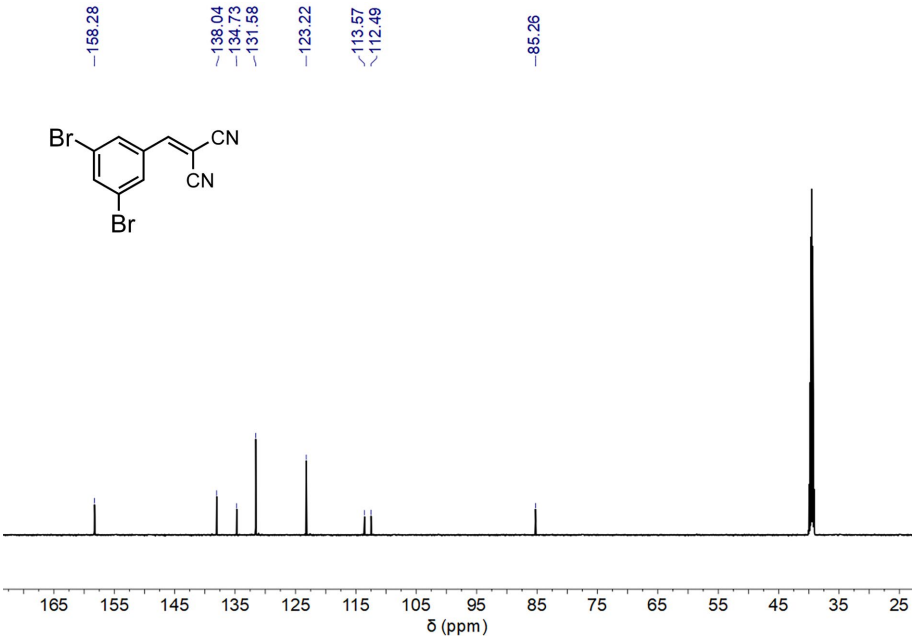

Fig. S38 ^{13}C NMR spectrum (150 MHz, DMSO-d_6, 298 K) of **3i**.

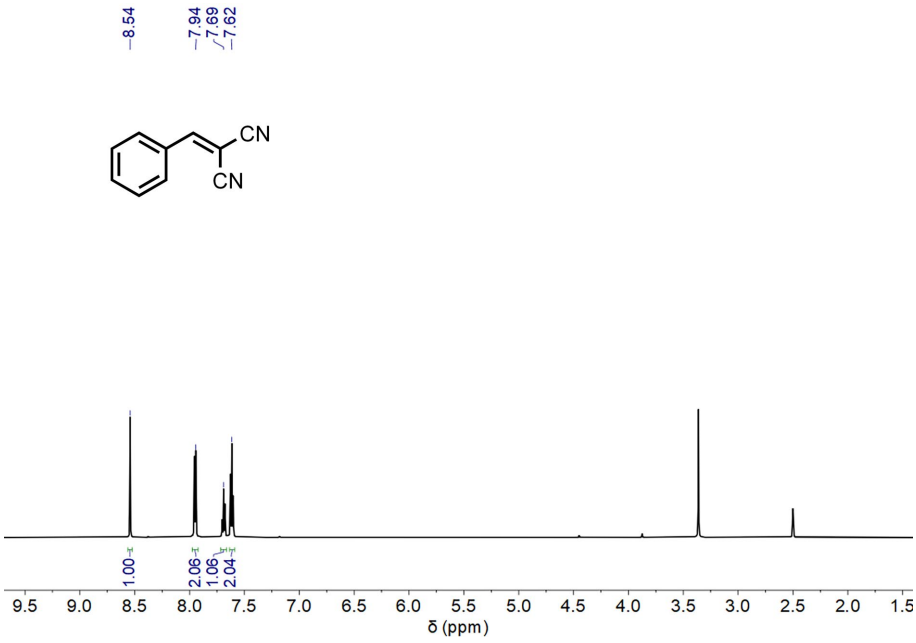

Fig. S39 ^{1}H NMR spectrum (600 MHz, DMSO-d_6, 298 K) of **3j**.

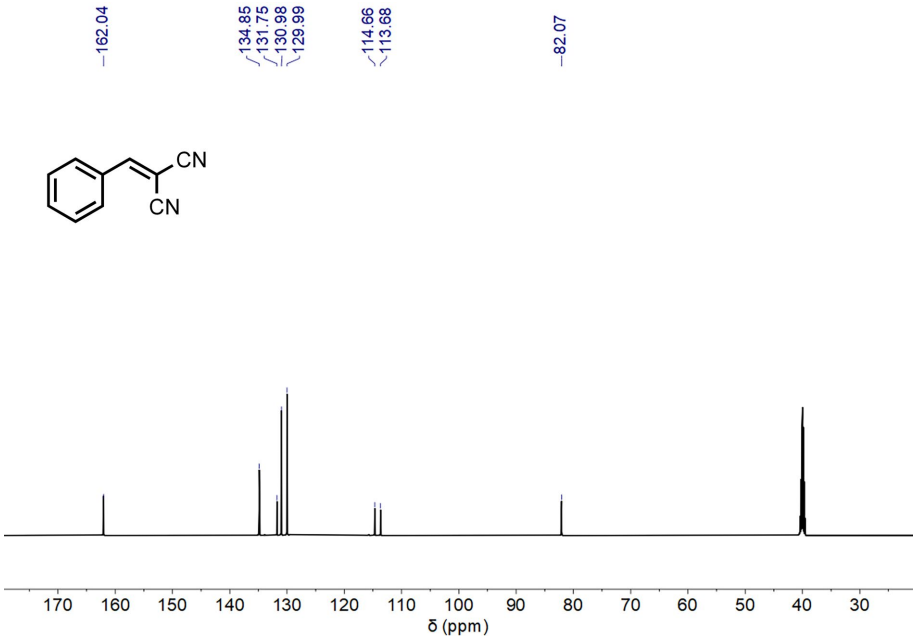

Fig. S40 ^{13}C NMR spectrum (150 MHz, DMSO-d_6, 298 K) of **3j**.

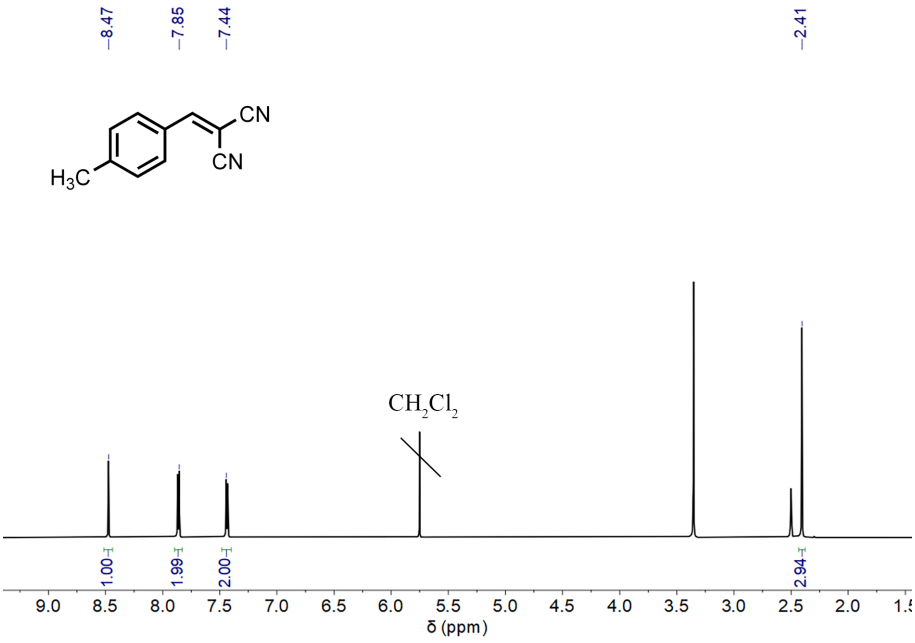

Fig. S41 ^{1}H NMR spectrum (600 MHz, DMSO-d_6, 298 K) of **3k**.

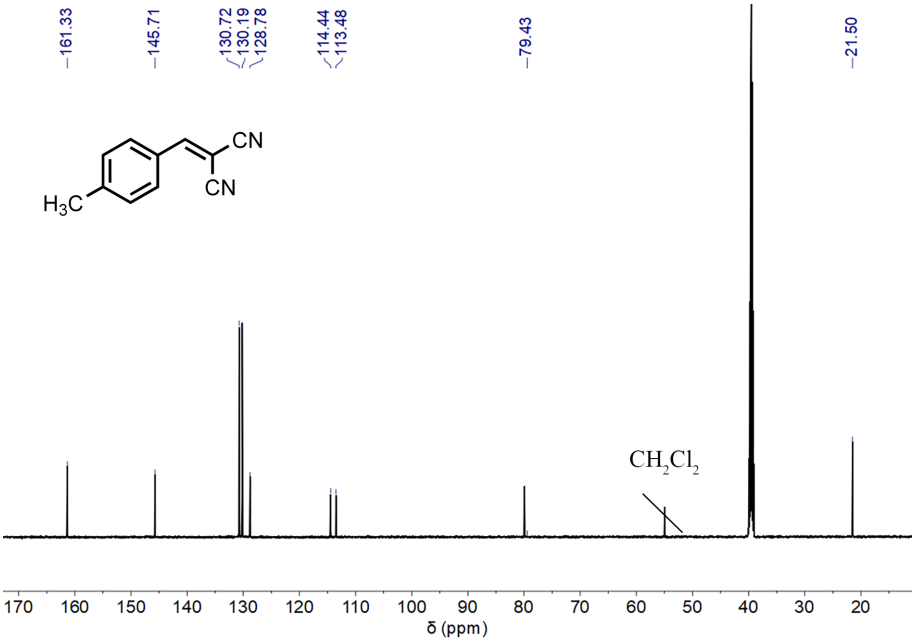

Fig. S42 ^{13}C NMR spectrum (150 MHz, DMSO-d_6, 298 K) of **3k**.

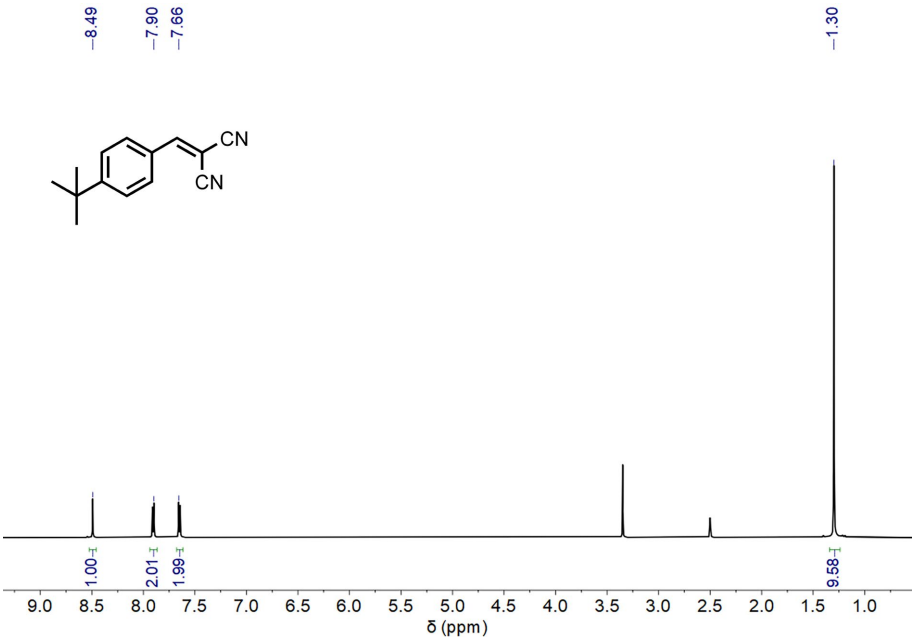

Fig. S43 ^{1}H NMR spectrum (600 MHz, DMSO-d_6, 298 K) of **3l**.

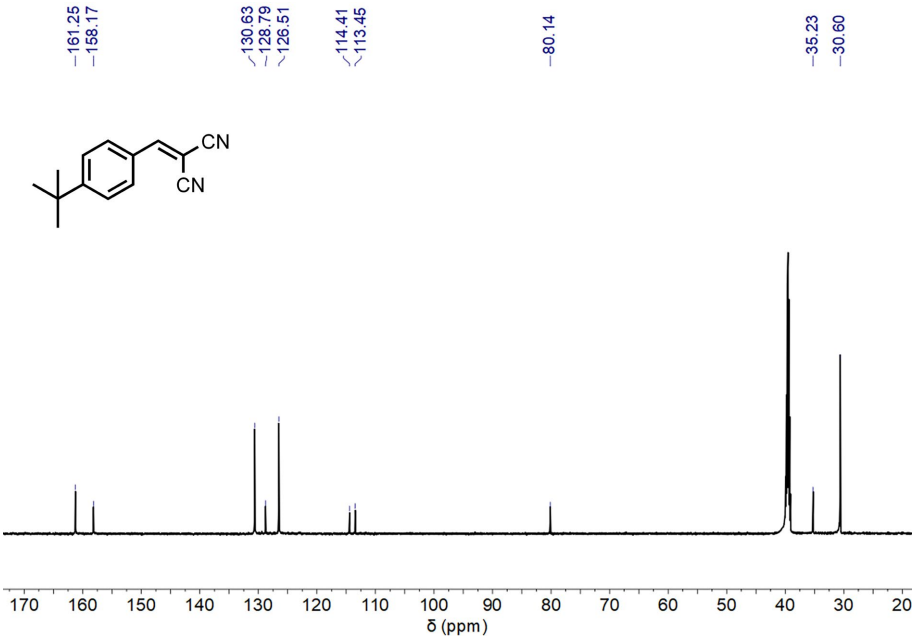

Fig. S44 ^{13}C NMR spectrum (150 MHz, DMSO-d_6, 298 K) of **3l**.

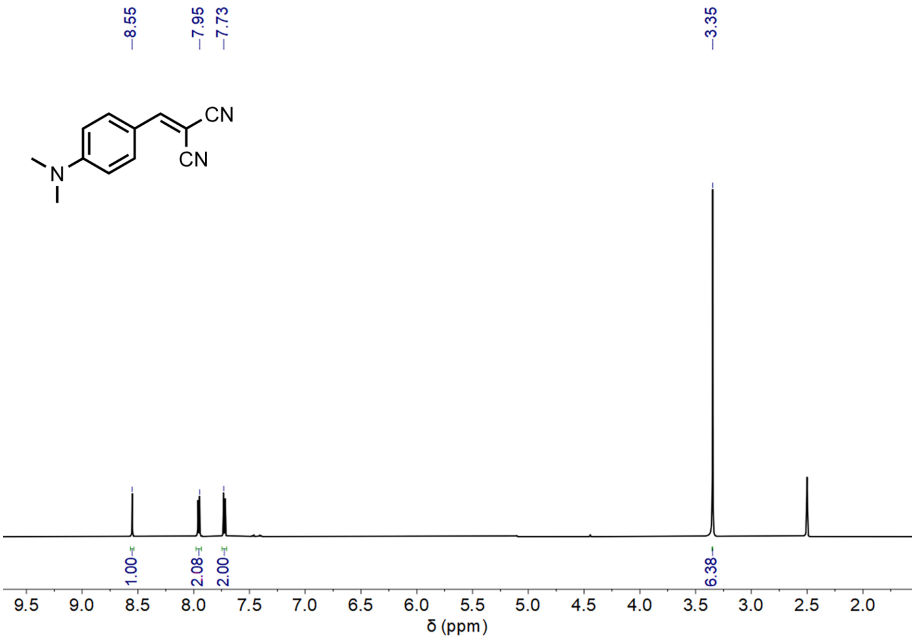

Fig. S45 ^{1}H NMR spectrum (600 MHz, DMSO-d_6, 298 K) of **3m**.

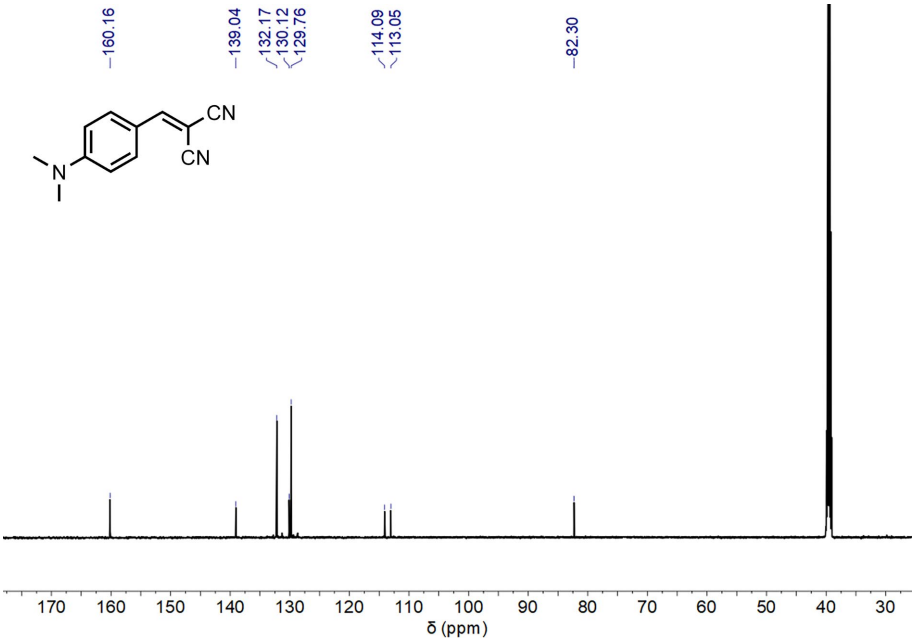

Fig. S46 ^{13}C NMR spectrum (150 MHz, DMSO-d_6, 298 K) of **3m**.

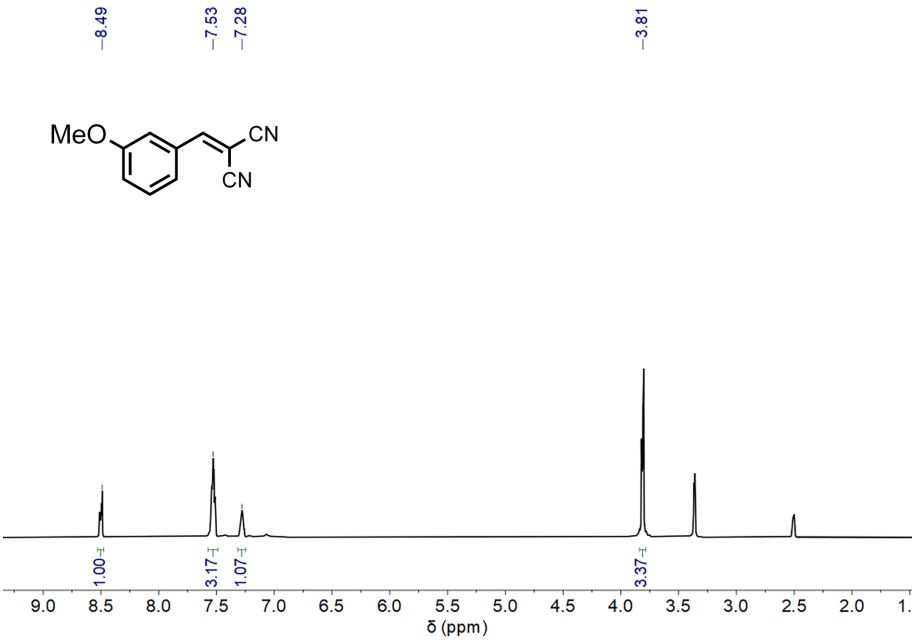

Fig. S47 ^{1}H NMR spectrum (600 MHz, DMSO-d_6, 298 K) of **3n**.

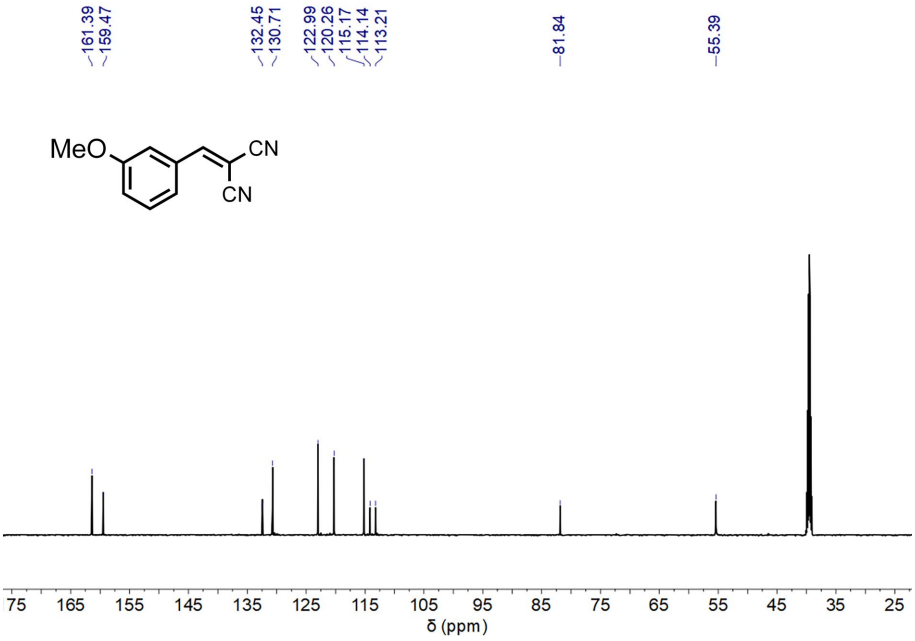

Fig. S48 ^{13}C NMR spectrum (150 MHz, DMSO-d_6, 298 K) of **3n**.

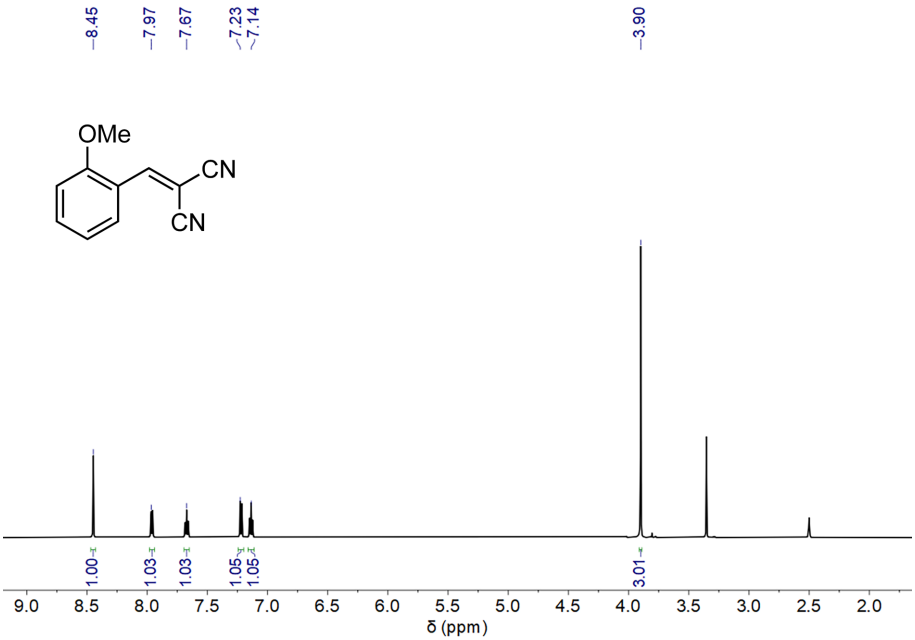

Fig. S49 ^{1}H NMR spectrum (600 MHz, DMSO-d_6, 298 K) of **3o**.

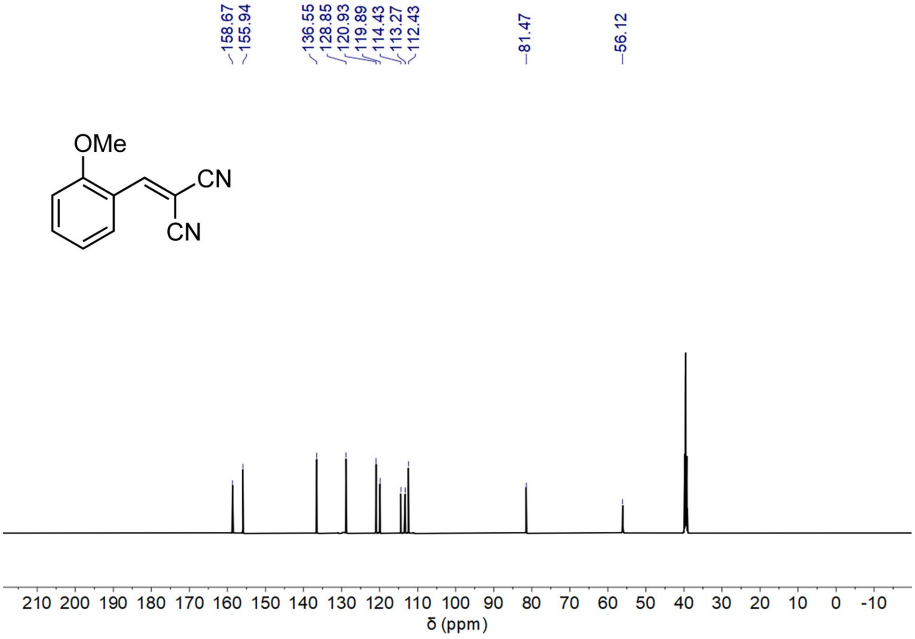

Fig. S50 ^{13}C NMR spectrum (150 MHz, DMSO-d_6, 298 K) of **3o**.

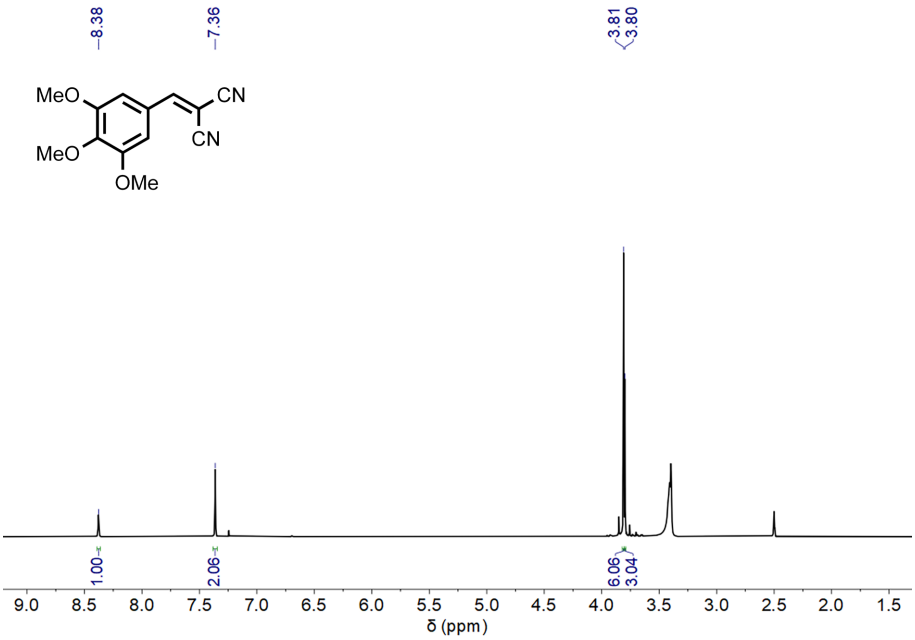

Fig. S51 ^{1}H NMR spectrum (600 MHz, DMSO-d_6, 298 K) of **3p**.

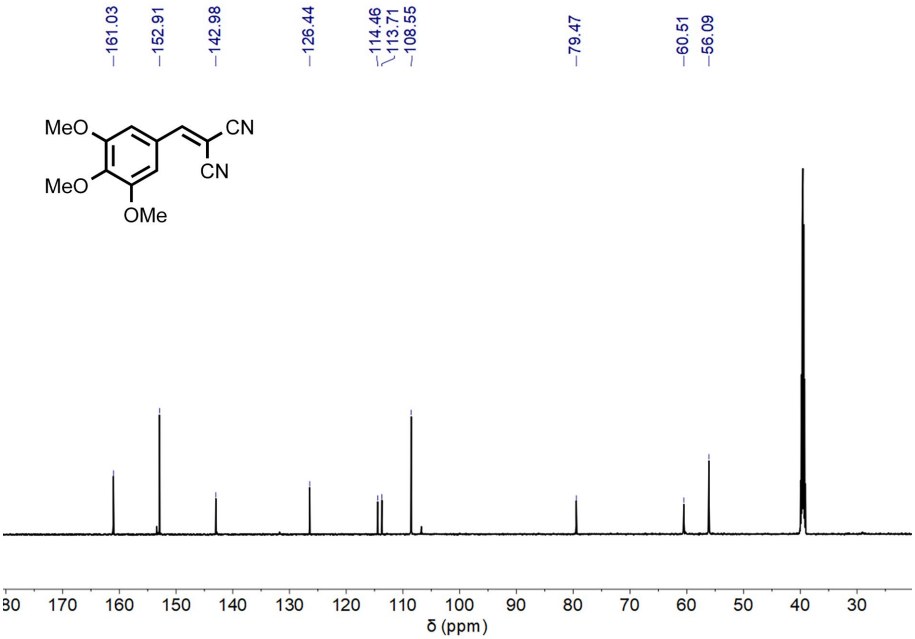

Fig. S52 ^{13}C NMR spectrum (150 MHz, DMSO-d_6, 298 K) of **3p**.

Table S2. Substrate scope of *γ*-butyrolactone derivatives.

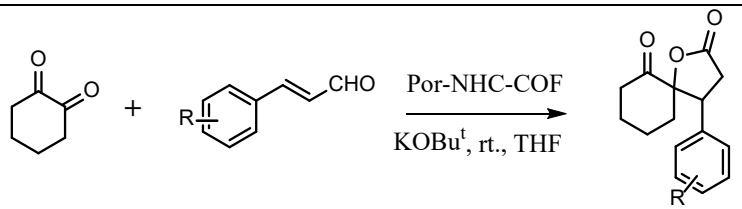

4 **5** **6**

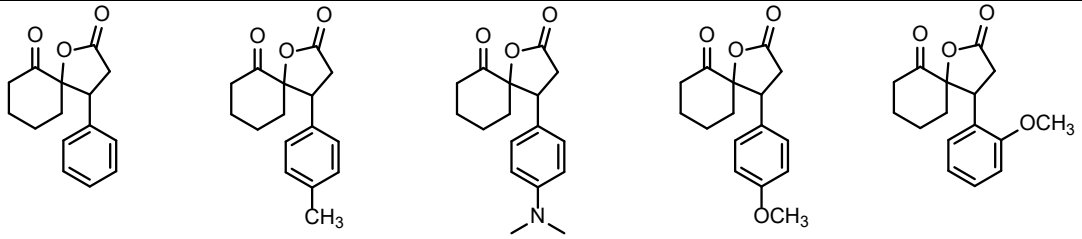

6a **6b** **6c** **6d** **6e**

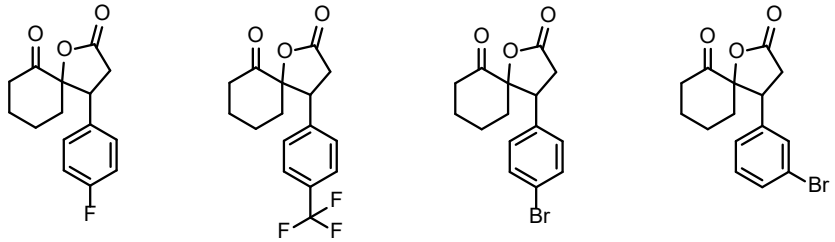

6f **6g** **6h** **6i**

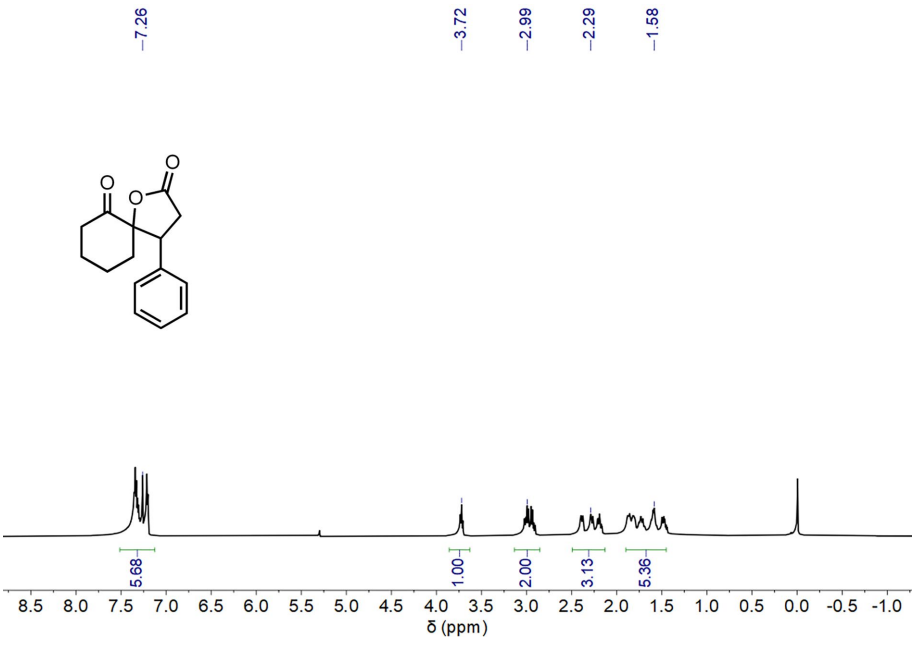

Fig. S53 ^{1}H NMR spectrum (600 MHz, $CDCl_3$, 298 K) of **6a**.

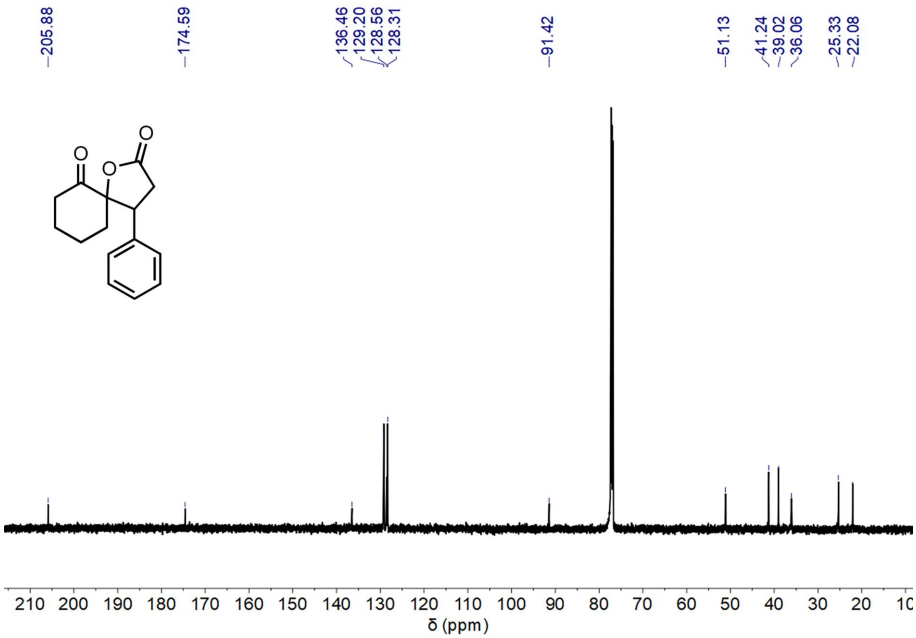

Fig. S54 ^{13}C NMR spectrum (150 MHz, $CDCl_3$, 298 K) of **6a**.

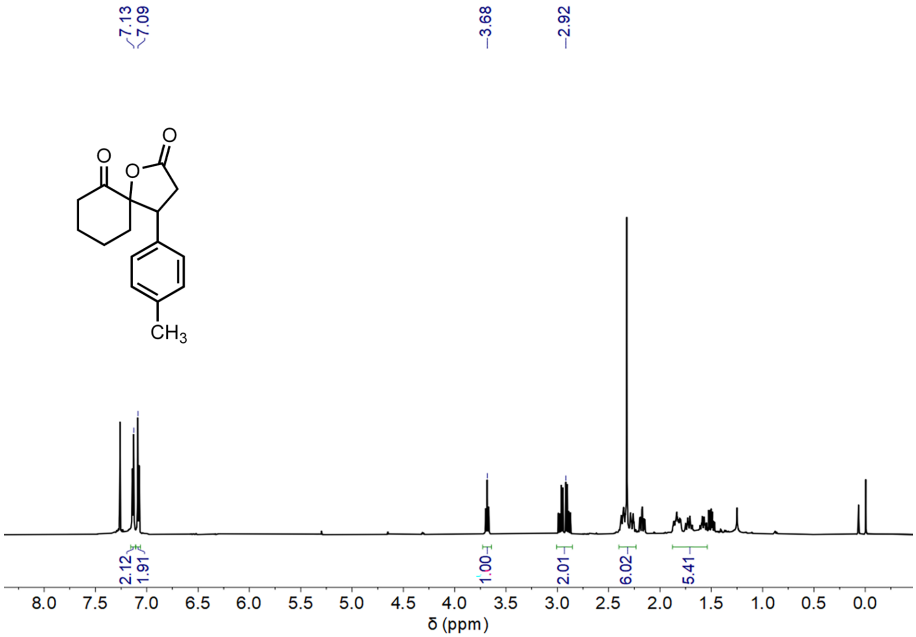

Fig. S55 ^{1}H NMR spectrum (600 MHz, $CDCl_3$, 298 K) of **6b**.

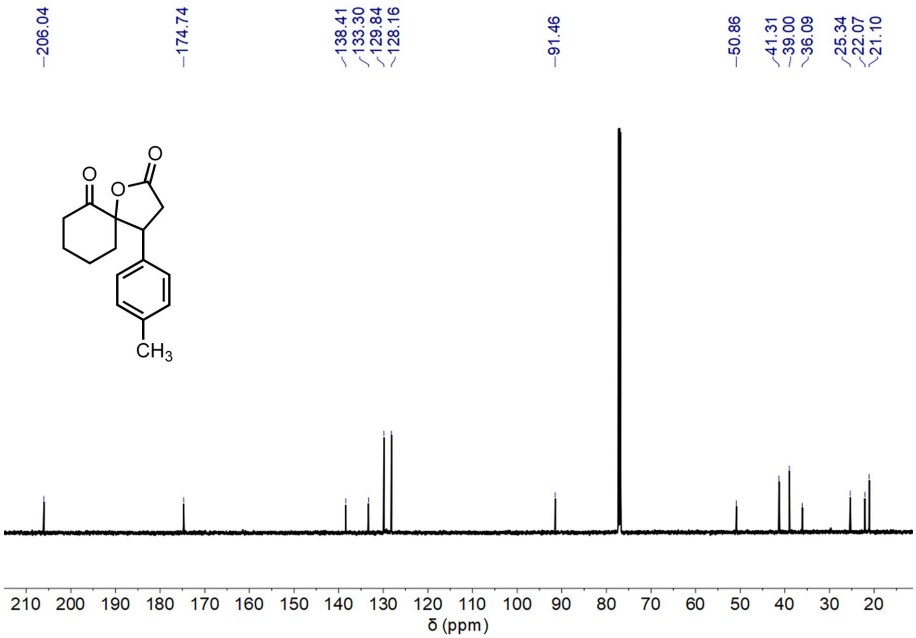

Fig. S56 ^{13}C NMR spectrum (150 MHz, $CDCl_3$, 298 K) of **6b**.

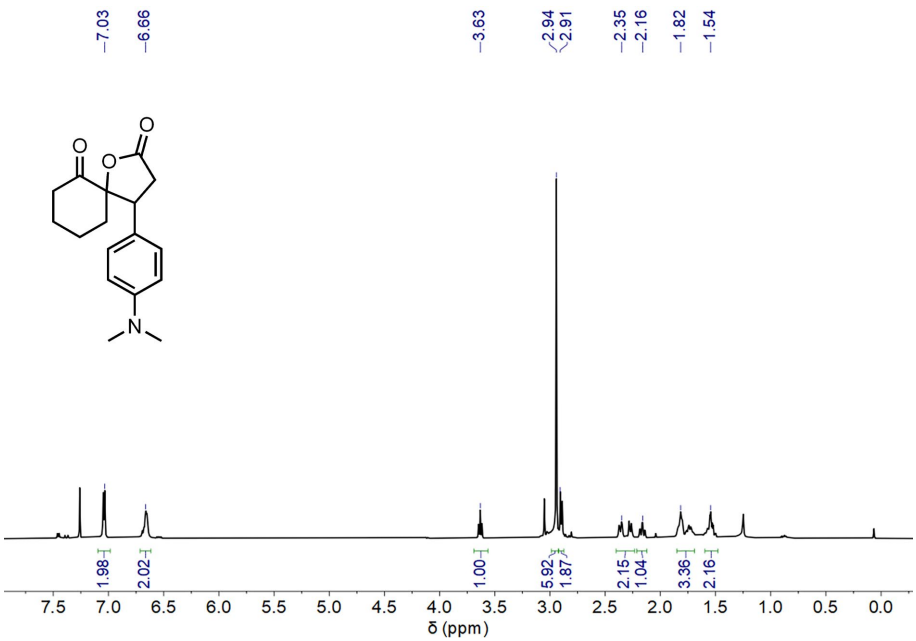

Fig. S57 ^{1}H NMR spectrum (600 MHz, $CDCl_3$, 298 K) of **6c**.

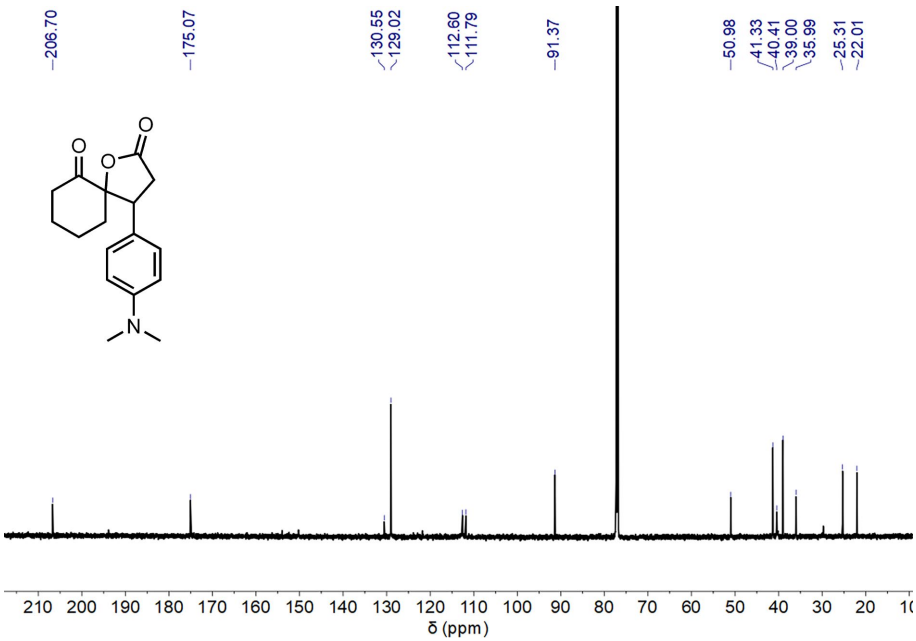

Fig. S58 ^{13}C NMR spectrum (150 MHz, $CDCl_3$, 298 K) of **6c**.

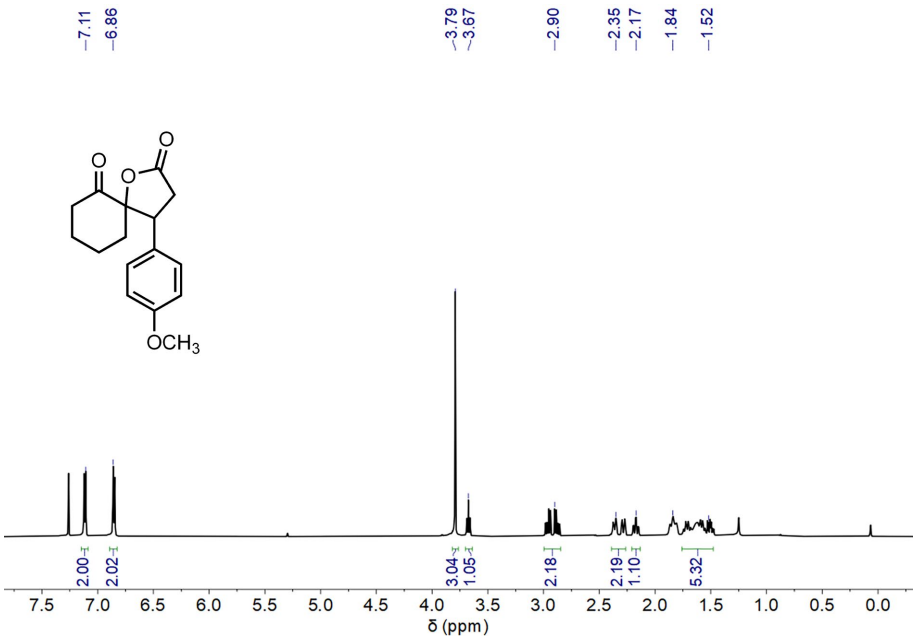

Fig. S59 ^{1}H NMR spectrum (600 MHz, $CDCl_3$, 298 K) of **6d**.

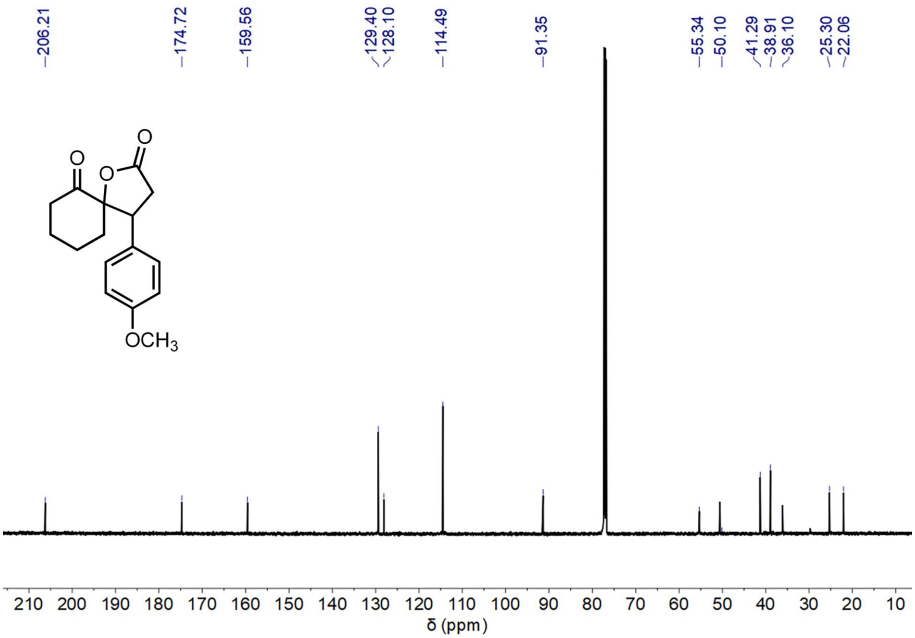

Fig. S60 ^{13}C NMR spectrum (150 MHz, $CDCl_3$, 298 K) of **6d**.

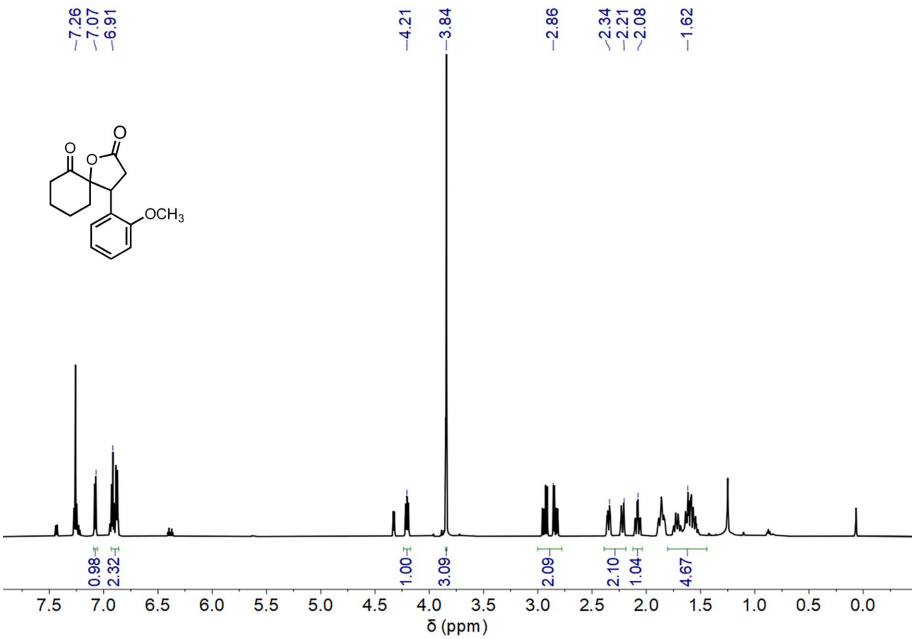

Fig. S61 ^{1}H NMR spectrum (600 MHz, $CDCl_3$, 298 K) of **6e**.

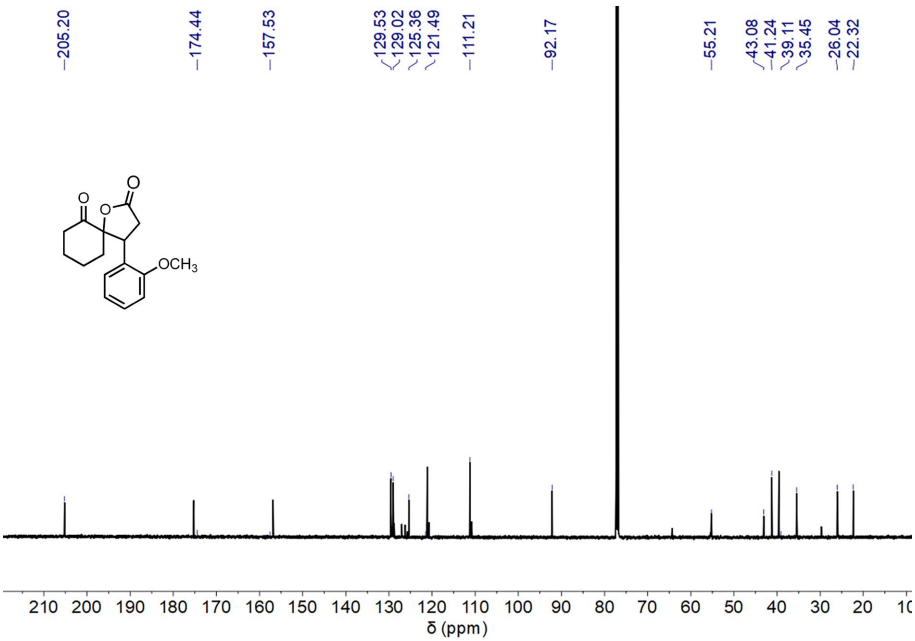

Fig. S62 ^{13}C NMR spectrum (150 MHz, $CDCl_3$, 298 K) of **6e**.

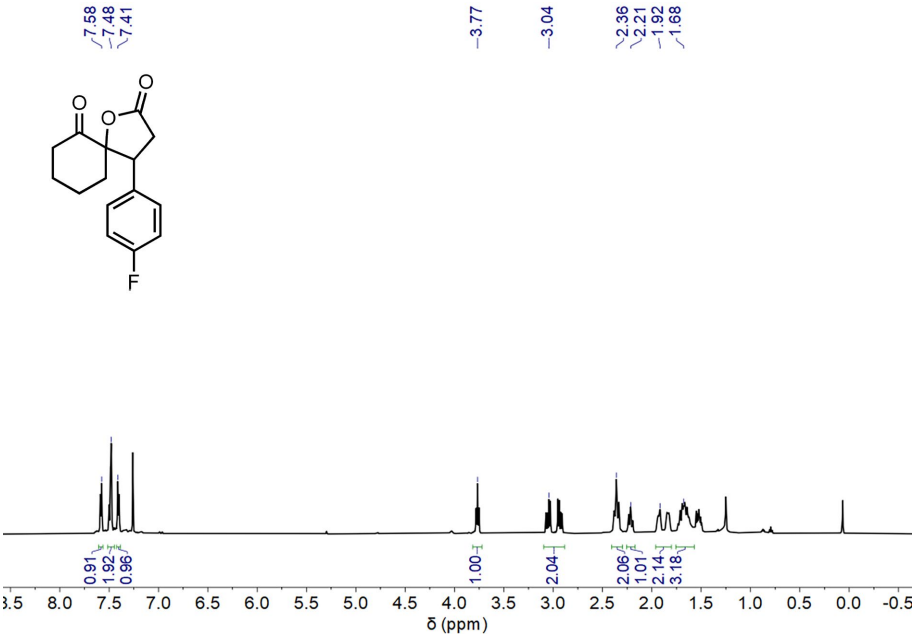

Fig. S63 ^{1}H NMR spectrum (600 MHz, $CDCl_3$, 298 K) of **6f**.

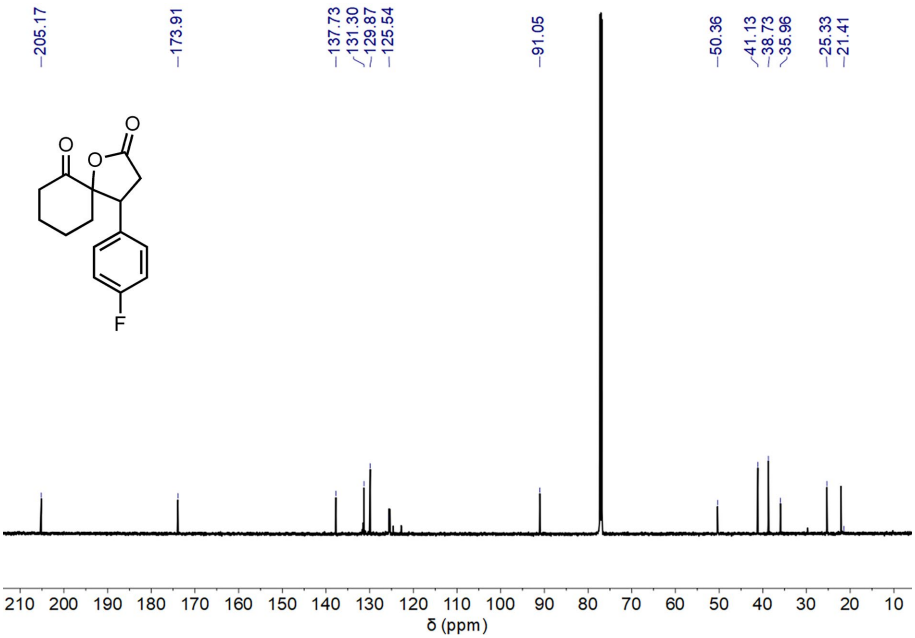

Fig. S64 ^{13}C NMR spectrum (150 MHz, $CDCl_3$, 298 K) of **6f**.

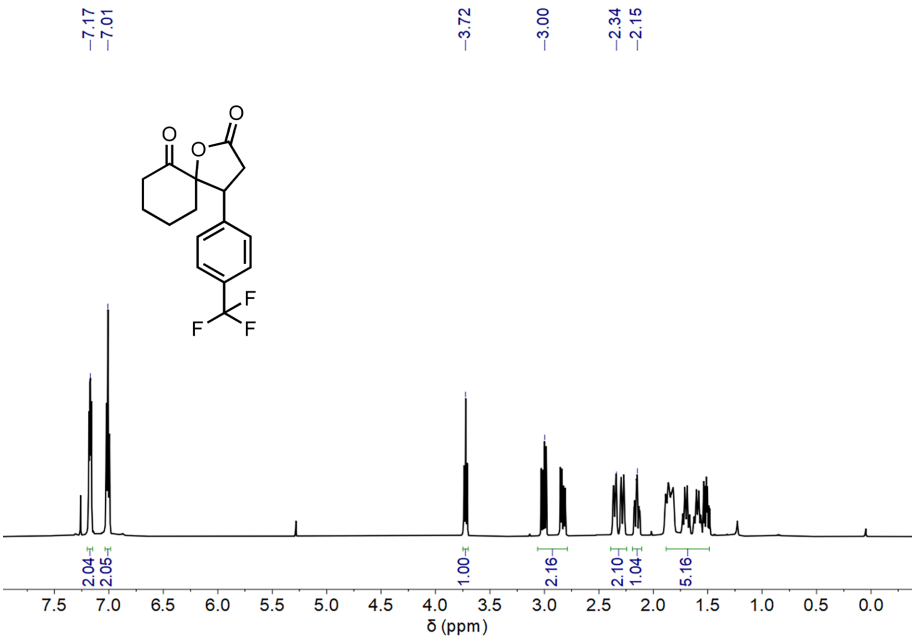

Fig. S65 ^{1}H NMR spectrum (600 MHz, $CDCl_3$, 298 K) of **6g**.

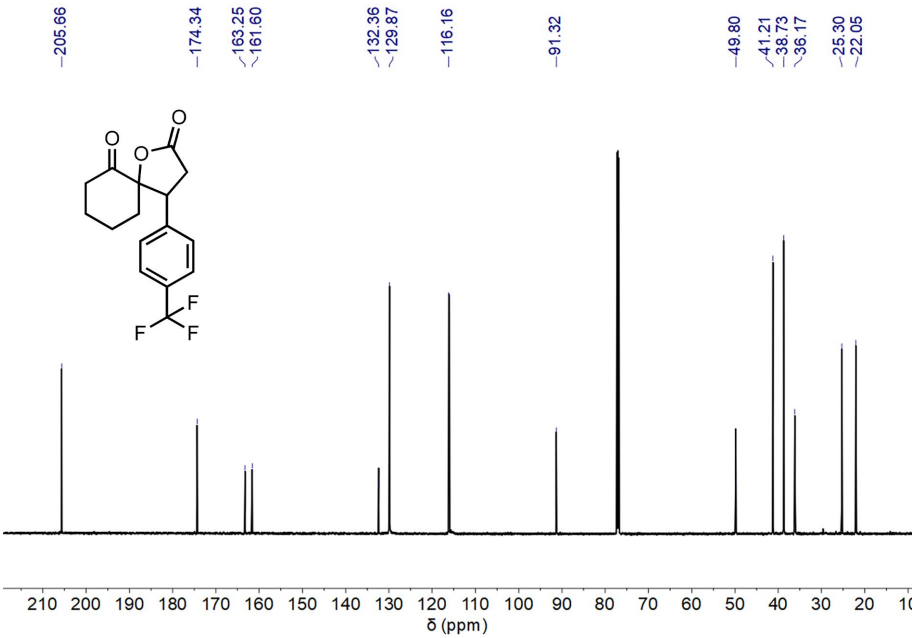

Fig. S66 ^{13}C NMR spectrum (150 MHz, $CDCl_3$, 298 K) of **6g**.

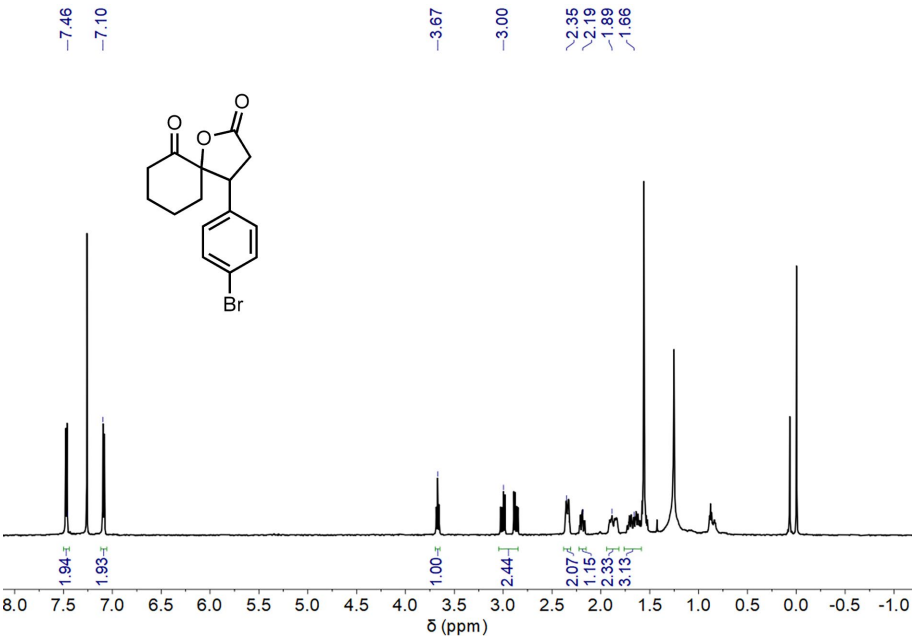

Fig. S67 ^{1}H NMR spectrum (600 MHz, $CDCl_3$, 298 K) of **6h**.

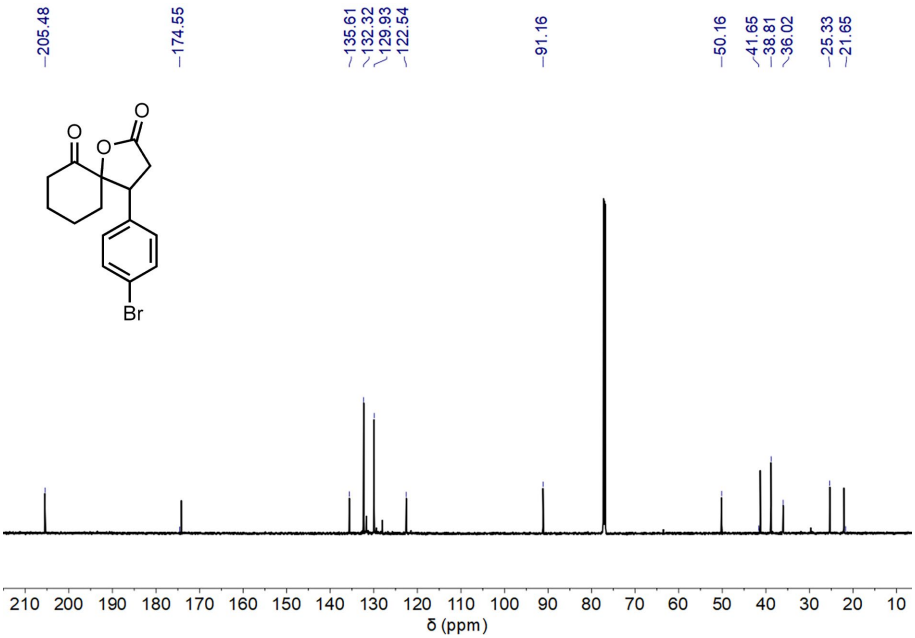

Fig. S68 ^{13}C NMR spectrum (150 MHz, $CDCl_3$, 298 K) of **6h**.

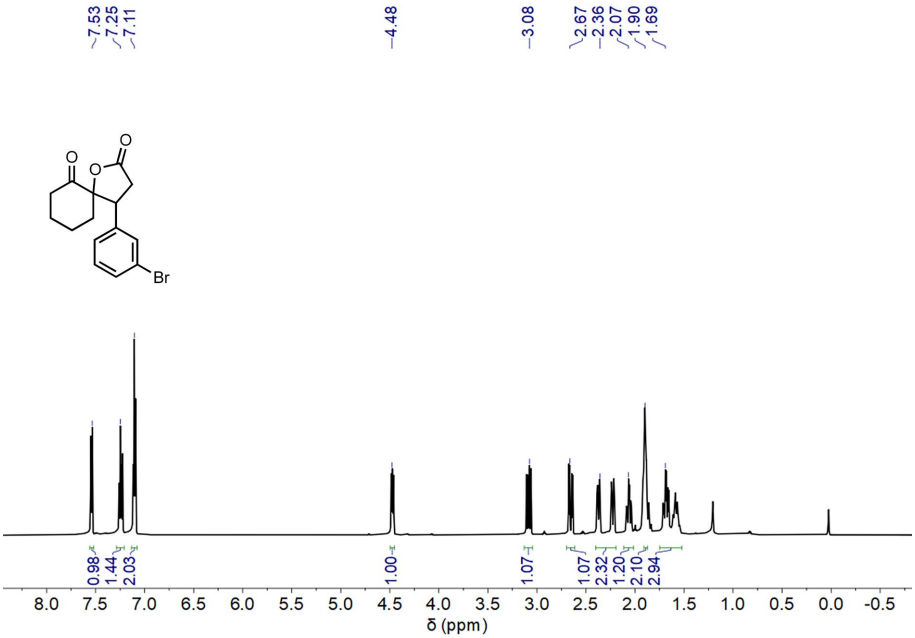

Fig. S69 ^{1}H NMR spectrum (600 MHz, $CDCl_3$, 298 K) of **6i**.

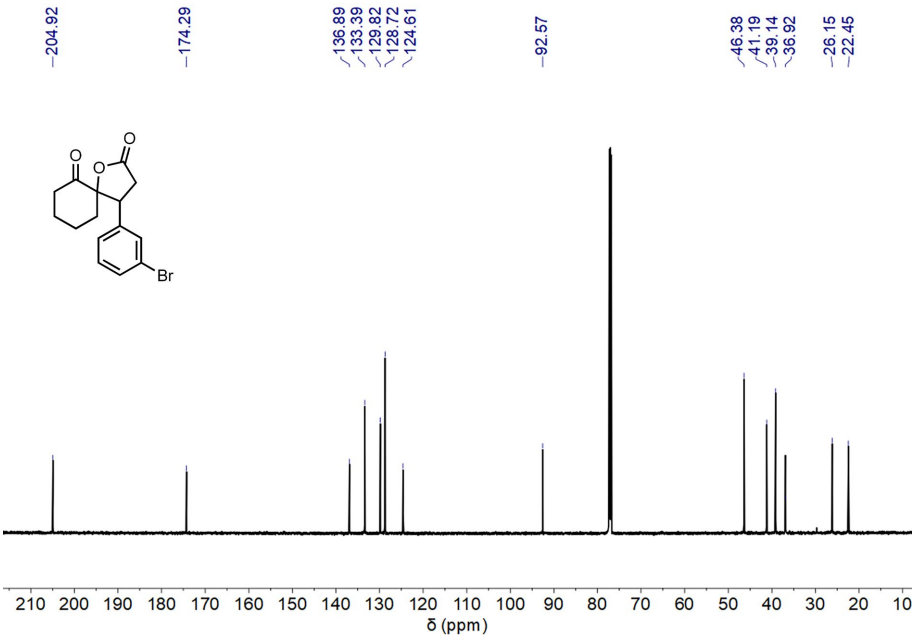

Fig. S70 ^{13}C NMR spectrum (150 MHz, $CDCl_3$, 298 K) of **6i**.

S6. References

1. D. Stay and M. C. Lonergan, Varying Anionic Functional Group Density in Sulfonate-Functionalized Polyfluorenes by a One-Phase Suzuki Polycondensation, *Macromolecules*, 2013, **46**, 4361-4369.
2. H. Sun, P. Ren and J. R. Fried, The COMPASS force field: parameterization and validation for phosphazenes, *Computational and Theoretical Polymer Science*, 1998, **8**, 229-246.
3. H. Sun, COMPASS: An ab Initio Force-Field Optimized for Condensed-Phase ApplicationssOverview with Details on Alkane and Benzene Compounds, *J. Phys. Chem. B*, 1998, **102**, 7338-7364.
4. D. S. m. BIOVIA, Materials Studio, 9.0, Dassault Syste`mes, San Diego, 2020.